Experimental confirmation of the two-source interference model for the fine structure of distortion product otoacoustic emissions

Carrick L. Talmadge
National Center for Physical Acoustics, University of Mississippi, University, Mississippi 38677

Glenis R. Long
Department of Audiology and Speech Sciences, Purdue University, West Lafayette, Indiana 47907

Arnold Tubis
Department of Physics, Purdue University, West Lafayette, Indiana 47907

Sumit Dhar
Department of Audiology and Speech Sciences, Purdue University, West Lafayette, Indiana 47907

(Received 26 June 1998; accepted for publication 21 September 1998)

High-resolution measurements of distortion product otoacoustic emissions (DPOAEs) from three different experimental paradigms are shown to be in agreement with the implications of a realistic ''two-source'' cochlear model of DPOAE fine structure. The measurements of DPOAE amplitude and phase imply an interference phenomenon involving one source in the region of strong nonlinear interaction of the primary waves (the strong ''overlap'' or generation region), and the other source region around the DPOAE tonotopic place. The component from the DPOAE place can be larger than the one from the generator region. These findings are supported by the analysis of the onset and offset of the DPOAE when the higher-frequency primary is pulsed on and off. The two-source hypothesis was further tested by adding a third tone closer in frequency to the DPOAE which modifies the amplitude of the component from the DPOAE place and leaves the one from the generator region unchanged. The results agree well with the model prediction that the variation with frequency, and implied latency, of the phase of the DPOAE tonotopic-place component are greater than the corresponding quantities for the component from the generation region. [S0001-4966(99)01101-7]

PACS numbers: 43.64.Bt, 43.64.Ha, 43.64.Jb [BLM]

INTRODUCTION

Distortion product otoacoustic emissions (DPOAEs) (Kemp, 1979) are signals measured in the ear canal which are generated in the cochlea through the nonlinear interaction of two external primary tones of frequencies f_1 and f_2 with $f_2 > f_1$. The distortion product (DP) energy originates in the region of maximum overlap of the cochlear excitations produced by the two primaries, which is near the tonotopic location of the f_2 primary (e.g., Kummer *et al.*, 1995). Because DPOAEs are vulnerable to ipsilateral and/or contralateral stimulation, ototoxic drugs, and physiological insults to the cochlea, it has been proposed (see, e.g., reviews in Robinette and Glattke, 1997) that DPOAEs may provide a clinically important tool for the measurement of the health status of the cochlea. However, the experimental evaluation of this proposal has revealed limitations in the effectiveness of DPOAEs as a clinical tool (reviewed in Gorga *et al.*, 1994). It has been argued that these limitations are associated with the quasiperiodic variations of DPOAE amplitude and phase with variations of DP frequency known as DPOAE fine structure (cf. Heitmann *et al.*, 1996).

This disparity between expectation and practice may be, in part, a result of the commonly held conception that the DPOAE levels are determined only by the health of the cochlea in the overlap region of the primaries (cf. Mills, 1997). This contrasts with recent claims that one DPOAE component originates from the place of generation in the overlap region, and the other comes from the DP wave component that travels apically from the overlap region, is reflected near the DP tonotopic site, and then travels basally to the ear canal (e.g., Kummer *et al.*, 1995; Brown *et al.*, 1996; Gaskill and Brown, 1996; Talmadge *et al.*, 1996, 1997, 1998). In this two-source model of DPOAEs, the DPOAE fine structure is the result of the interference between these two cochlear sources. The general concept of such a disparate-place two-source model of DPOAEs was first proposed by Kemp and Brown (1983), although they did not specify the origin of the second DPOAE source.

Several pictures of the multiple sources of DPOAEs have been proposed. Input–output functions of DPOAEs in many species have a distinct and significant notch around primary levels of 55–70 dB SPL (reviewed in Mills, 1997). DPOAEs were proposed to be dominated by one source when the primary levels were below 55 to 60 dB SPL and a second source at higher primary levels. The notch in the input–output functions was interpreted as the result of phase cancellation between the two components. The idea of two level-dependent sources was supported by the differential vulnerability of DPOAEs that are produced by low-level and high-level primaries. DPOAEs generated with low-level pri-

maries have been universally found to be more vulnerable to insults such as administration of loop diuretics, aminoglycosides, induction of asphyxia, and even death, than those generated by higher-level primaries (reviewed in Mills, 1997). In these models, both components were hypothesized to come from the overlap region of the primaries. Any change in position of origin on the basilar membrane was assumed to stem from the changing shape of the traveling wave with level.

Recent modeling advances (Talmadge *et al.*, 1997, 1998) suggest that the disparate-place two-source picture is a general feature of any transmission line model of DPOAEs that has realistic basilar-membrane activity patterns and a low level of distributed inhomogeneities along the cochlear partition. In addition, it was concluded in these studies that for experiments in which the frequency ratio f_2/f_1 is held fixed while the DP frequency is varied, the DPOAE source component arising from the overlap region (termed hereafter the ''overlap-region'' component) would have a short latency and slow phase variation with DPOAE frequency. In contrast, the DPOAE component arising from cochlear reflection (termed hereafter the ''reflection-site'' component) would be expected to have a long latency and a rapid phase variation with DPOAE frequency. It is this difference in the phase variation of the two components that gives rise to DPOAE fine structure. A less straightforward further implication of the model relates to the relative amplitudes of the two components. The overlap-region component will not necessarily have a larger magnitude than the reflection-site component, even if $|R_a(\omega_{\mathrm{dp}})|$, the magnitude of the coefficient for reflectance around the DP tonotopic site (e.g., Talmadge *et al.*, 1998 and Sec. I A of this paper), is less than 1. These modeling results suggest that, in fact, DPOAEs constitute a much more complex cochlear phenomena than was originally contemplated, and this complexity may explain the lack of agreement in many cases between DPOAE and audiometric evaluations of cochlear status. Some of the essential features of these cochlear models will be reviewed in Sec. I below.

The question of a possible two-source model is explored in this paper using a number of experimental paradigms. In the two-source model of Talmadge *et al.* (1998), the rapidly varying phase of the reflection-site component makes it the main determinant of the frequency spacing of DPOAE fine structure. Consequently, in experimental measurements of multiple orders of DPOAEs, in which the frequency of the f_2 primary is held fixed, it is expected (Piskorski, 1997; Talmadge *et al.*, 1997, 1998) and observed that amplitude fine-structure maxima and minima of the varying orders of DPOAEs will approximately line up when DPOAE level is plotted versus DP frequency. Similarly, when the DPOAE frequency is held fixed and DPOAE level is plotted versus f_2 frequency, no significant fine structure is either expected or observed (Piskorski, 1997). These data provide strong, although somewhat indirect, tests of the two-source DPOAE model.

Other indirect evidence for two cochlear sources comes from the methodology of Brown *et al.* (1996), which is based on the assumption that two cochlear sources give DPOAE contributions with very different phase dependencies on the DPOAE frequency. Their study does not directly probe the basilar-membrane location of the component with the rapid phase variation, nor indicate whether or not this more rapidly varying component arises from a cochlear source region which is different from that of the slowly varying component. However, Brown *et al.* (1996) note that the different group delays suggest different places of origin. A further analysis technique proposed by Stover *et al.* (1996) offers the possibility of extracting the group delays of the fast- and slow-phase terms by inverse Fourier-transforming DPOAE amplitude and phase data that is obtained using the fixed f_2 paradigm. While suggestive of the possibility of two sources, the evidence of two sources provided by the data is indirect and somewhat difficult to interpret theoretically.

More direct evidence of the presence of two components is obtained by introducing a third tone as a suppressor close in frequency to the DPOAE, as was done by Kemp and Brown (1983), Kummer *et al.* (1995), Gaskill and Brown (1996) and Heitmann *et al.* (1997, 1998). The DPOAE fine structure was either decreased or entirely removed when a suppressor tone was introduced near in frequency to the DPOAE (Heitmann *et al.*, 1997, 1998). If the DPOAE were entirely rooted in the overlap region, this effect on DPOAE fine structure would not be expected from the introduction of such a suppressor tone.

In this paper, further evidence is presented in support of a two-source model of the type described in Talmadge *et al.* (1998). After the model is briefly summarized, it is applied to the case of fixed frequency-ratio DPOAE measurements. Here, the overlap-region component will have a phase which slowly varies with DP frequency, whereas the reflection-site component will have a more rapid phase variation. The resulting variations of DPOAE amplitude and phase with frequency are shown to provide a unique signature that can only be explained in terms of the interference of two components. Furthermore, the variation of the DPOAE phase with frequency for the case in which the overlap-region component is dominant is expected to be categorically different from the case in which the reflection-site component is dominant. For the case of a suppressor tone of varying level and close in frequency to the DPOAE, it is predicted that the relative contribution of the two components can be manipulated so as to allow for the transition from the case in which the reflection-site component is dominant to the one in which the overlap-region component is dominant.

A further test of this two-source model is provided by observing the temporal behavior of a DPOAE when one of its primaries is pulsed and the other is kept on continuously. This test is a variation of the one originally introduced by Whitehead *et al.* (1996). The predictions of this two-source model again indicate that the behaviors of the DPOAE amplitude and phase, in which one or the other source component is dominant, will be categorically different. As in the case of the fixed frequency-ratio, continuous-tone paradigm, when a suppressor tone is added, it is predicted that a transition in the observed temporal amplitude and phase behavior can be achieved. This type of experimental result would be extremely difficult to obtain in a single-source model of

DPOAE fine structure (e.g., Sun *et al.*, 1994a, b). Furthermore, since the two source contributions are expected to have very different latencies, one should also be able to unambiguously observe the short-latency component associated with the overlap region, either by itself or in combination with the long-latency component associated with the reflection site.

The model of Talmadge *et al.* (1998) is briefly described in Sec. I. The predictions of the model which are relevant to the experiments discussed in this paper are repeated in a less mathematical form in the description of the experiments (Secs. III–V).

I. MODEL

A. Overview

The underlying cochlear model is assumed to have a time-delayed stiffness feedback of the form suggested by Zweig (1991) in order to give realistic ''tall and broad'' activity patterns, together with the low-level distributed basilar-membrane roughness of the form suggested by Zweig and Shera (Shera and Zweig, 1993; Zweig and Shera, 1995), which gives rise to the apical reflectance responsible for the fine structure of otoacoustic emissions and threshold microstructure (Zweig and Shera, 1995; Talmadge *et al.*, 1996, 1997, 1998). The basilar membrane is also assumed to have a nonlinearity in damping, which is associated with the finite power level of the transduction mechanisms of the outer-hair cells responsible for cochlear amplification.

As was discussed in the Introduction, the disparate-place two-source model features the interference between two ear-canal components of the DPOAE which originate from different regions in the cochlea. In this model, the nonlinear interactions of the excitations created by the two primary tones of (angular) frequencies ω_1 and ω_2 $(\omega_2>\omega_1)$ generate DP waves in the cochlea of frequencies $\omega_{\rm dp}=(n+1)\omega_1-n\omega_2$ $(n=1,2,3,...)$. For the case of continuous-primary-tone and an apical DPOAE (i.e., one whose frequency corresponds to a tonotopic site apical to the overlap region, so that $\omega_{\rm dp}<\omega_1<\omega_2$), the two-source model prediction for the (complex) DPOAE wave amplitude can be written in the analytic form (Talmadge *et al.*, 1998):

$$P_e(\omega_2,\omega_2/\omega_1,\omega_{\rm dp}) = \frac{P_l(\omega_2,\omega_2/\omega_1,\omega_{\rm dp})+R_a(\omega_{\rm dp})P_r(\omega_2,\omega_2/\omega_1,\omega_{\rm dp})}{1-R_a(\omega_{\rm dp})R_b(\omega_{\rm dp})}. \tag{1}$$

Here, $P_l(\omega_2,\omega_2/\omega_1,\omega_{\rm dp})$ is the (complex) amplitude of the overlap-region contribution to the ear-canal pressure, the product $R_a(\omega_{\rm dp})P_r(\omega_2,\omega_2/\omega_1,\omega_{\rm dp})$ is the amplitude of the reflection-site contribution to the ear-canal pressure, and $R_a(\omega_{\rm dp})$ and $R_b(\omega_{\rm dp})$ are, respectively, the cochlear apical and basal reflectances. The quantity $P_r(\omega_2,\omega_2/\omega_1,\omega_{\rm dp})$ gives the ear-canal contribution from the reflection-site component in the limit that $R_a(\omega_{\rm dp})\to 1$ and $R_b(\omega_{\rm dp})\to 0$. If the auditory periphery were completely scale invariant, then the dependence of the complex amplitudes P_l and P_r on frequency would reduce to $P_l(\omega_2/\omega_1,\omega_{\rm dp})$ and $P_r(\omega_2/\omega_1,\omega_{\rm dp})$.

The precise meanings of $R_a(\omega)$ and $R_b(\omega)$ are given in relation to the trans-partition pressure wave near the cochlear base for the case of the complex time harmonic behavior $e^{i\omega t}$ (Talmadge *et al.*, 1998). In the case of external driving at frequency ω, the spatial part of this pressure is proportional to

$$\psi_r(x,\omega)+R_a(\omega)\psi_l(x,\omega), \tag{2}$$

where x is the distance from the cochlear base. In the case of no external driving (as is appropriate, e.g., for DPOAEs), it is proportional to

$$R_b(\omega)\psi_r(x,\omega)+\psi_l(x,\omega). \tag{3}$$

The right- and left-moving basis functions, $\psi_r(x,\omega)$ and $\psi_l(x,\omega)$, are normalized to 1 at $x=0$, and are given to a good approximation by the Wentzel–Kramers–Brillouin (WKB) approximations (e.g., Mathews and Walker, 1964; Zweig *et al.*, 1976):

$$\psi_r(x,\omega)=\sqrt{\frac{k(0,\omega)}{k(x,\omega)}}\exp\left\{-i\int_0^x k(x',\omega)dx'\right\}, \tag{4}$$

$$\psi_l(x,\omega)=\sqrt{\frac{k(0,\omega)}{k(x,\omega)}}\exp\left\{+i\int_0^x k(x',\omega)dx'\right\}, \tag{5}$$

where $k(x,\omega)$ is the local cochlear wave number. It should be noted that $R_b(x,\omega)$ is mainly determined by the dynamics of the middle ear and the ear canal, and $R_a(\omega)$ is determined by the apical reflections of the cochlear wave, which are concentrated around the tonotopic site for frequency ω.

The reflection-site DPOAE component was parameterized in Eq. (1) so as to emphasize that the ear-canal contribution from this component vanishes in the absence of apical reflections (e.g., $|R_a|\to 0$). Furthermore, the denominator term, $1-R_a(\omega_{\rm dp})R_b(\omega_{\rm dp})$, was left as a separate term, instead of being absorbed into the definitions of P_l and P_r, in order to directly parameterize the effects of the cochlear resonance arising from multiple internal reflections from the tonotopic region and the base of the cochlea (Talmadge *et al.*, 1998). Consequently, the P_l and P_r terms include just the effects of forward transmission through the outer/middle ear of the primary waves, with the level of nonlinear interaction giving rise to apically and basally moving DP traveling waves of differing amplitudes originating in the overlap region, and reverse transmission through the outer/middle ear at the DP frequency.

The main features of the dependence of $R_a(\omega_{\rm dp})$ and $R_b(\omega_{\rm dp})$ on $\omega_{\rm dp}$ can be determined using the results from Zweig and Shera (Shera and Zweig, 1993; Zweig and Shera, 1995) and Talmadge *et al.* (1998). Zweig and Shera were the first to point out the phenomena of ''dynamic symmetry creation,'' which results in a phase dependence of R_a given by

$$\arg[R_a(\omega_{\rm dp})]\cong\varphi_a+\hat{k}(\omega_{\rm dp})\hat{x}(\omega_{\rm dp}) \cong\varphi_a-\frac{\hat{k}(\omega_{\rm dp})}{k_\omega}\log\left(\frac{\omega_{\rm dp}}{\omega_0}\right), \tag{6}$$

where ω_0 is the tonotopic frequency of the basilar membrane at the base of the cochlea, $\hat{k}(\omega_{dp})$ is the wave number of the ω_{dp} traveling wave at the amplitude maximum of the activity pattern, and k_ω is a parameter in the cochlear frequency-place map,

$$\hat{x}(\omega_{dp}) \cong -(1/k_\omega)\log(\omega_{dp}/\omega_0). \tag{7}$$

As a consequence of the fact that apical reflectance arises from spatial filtering of distributed roughness, the expected value of $|R_a|$ will depend on the average roughness in the vicinity of the activity-pattern maximum. Because the amount of roughness may vary with position, this will result in a dependence of $|R_a|$ on frequency. In direct analogy to bandpass filtering of white noise in the time domain, the amplitude of $|R_a|$ will fluctuate with ω_{dp} [or equivalently $\hat{x}(\omega_{dp})$], with a correlation length in the fluctuations given by the bandwidth of the spatial filter, which in turn can be related to the width of the activity-pattern peak region.

B. Application of the model to fixed frequency-ratio measurements

The fixed frequency-ratio continuous-tone paradigm has a simplified theoretical interpretation relative to other DPOAE measurement paradigms. This is a result of the approximate scale invariance of the auditory periphery. The consequence of this approximate symmetry is that, for a given value of $r=\omega_2/\omega_1$, $P_l(r,\omega_{dp})$ and $P_r(r,\omega_{dp})$ will have slow phase variations with ω_{dp}.

A rough argument for this slow phase variation may be easily given. If the sound transducer voltage for two periodic signals ω_1 and ω_2 is

$$V(t)=A\cos\omega_1 t + B\cos\omega_2 t, \tag{8}$$

then the pressure variation of the cochlear wave at the $f_2=\omega_2/2\pi$ tonotopic place $\hat{x}(\omega_2)$, in the absence of nonlinearities, will be

$$P(t)\propto \tilde{A}\cos(\omega_1 t+\varphi(\omega_1,\hat{x}(\omega_2))+\varphi_1) + \tilde{B}\cos(\omega_2 t+\varphi(\omega_2,\hat{x}(\omega_2))+\varphi_2), \tag{9}$$

with

$$\varphi(\omega,\hat{x}(\omega_2)) \cong -\int_0^{\hat{x}(\omega_2)} dx\,\frac{2\pi}{\lambda(\omega,x)}, \tag{10}$$

where $2\pi/\lambda(\omega,x)$ is the real part of the cochlear traveling wave number $k(x,\omega)$. The assumption of scale invariance may be conveniently expressed by

$$\lambda(\omega,x)=\lambda\left(\frac{\omega}{\hat{\omega}(x)}\right), \tag{11}$$

where $\hat{\omega}(x)$ is the tonotopic (angular) frequency at location x along the basilar membrane,

$$\hat{\omega}(x)=\omega_0 e^{-k_\omega x}. \tag{12}$$

For a cochlear nonlinearity of order $2n+1$ in the neighborhood of $x=\hat{x}(\omega_2)[\equiv(1/k_\omega)\log(\omega/\omega_0)]$, the phase of the ω_{dp} DPOAE measured in the ear canal φ_e will be given approximately by

$$\varphi_e(\omega_{dp}) = -(n+1)\int_0^{\hat{x}(\omega_2)} dx\,\frac{2\pi}{\lambda(\omega_1/\hat{\omega}(x))} + n\int_0^{\hat{x}(\omega_2)} dx\,\frac{2\pi}{\lambda(\omega_2/\hat{\omega}(x))} - \int_0^{\hat{x}(\omega_2)} dx\,\frac{2\pi}{\lambda(\omega_{dp}/\hat{\omega}(x))}, \tag{13}$$

where the upper limit of integration has been set at the tonotopic location of the higher primary $\hat{x}(\omega_2)$—the approximate center of the overlap region. If the long-wave assumptions,

$$\frac{2\pi}{\lambda(\omega_1/\hat{\omega}(x))} \cong \text{const.}\ \frac{\omega_1}{\hat{\omega}(x)}, \tag{14}$$

$$\frac{2\pi}{\lambda(\omega_{dp}/\hat{\omega}(x))} \cong \text{const.}\ \frac{\omega_{dp}}{\hat{\omega}(x)}, \tag{15}$$

are made in Eq. (13), and it is noted that from scale invariance the second integral in Eq. (13) is very nearly independent of ω_2, it follows that $\varphi_e(\omega_{dp})$ is approximately only a function of the ratio ω_2/ω_1, and is thus very slowly varying with ω_{dp} for constant frequency ratios.

Based on these arguments, one is led to the prediction that the overlap-region component P_l in Eq. (1) will vary weakly with ω_{dp}, whereas the reflection-site component $R_a P_r$ will have a rapidly varying phase and a slowly varying magnitude, with the dominant phase variation in the second term arising from the phase variation of R_a. From Eq. (1), the amplitudes and phases of the total DPOAE signal and its two components (including the effects of the reflections at the cochlear base and DP tonotopic site) are given by the following notation:

$$a_e(\omega_{dp})=|P_e|,\quad a_{nl}(\omega_{dp})=\left|\frac{P_l}{1-R_aR_b}\right|,$$
$$a_{refl}(\omega_{dp})=\left|\frac{R_aP_r}{1-R_aR_b}\right|, \tag{16}$$
$$\varphi_e(\omega_{nl})=\arg(P_e),\quad \varphi_{nl}(\omega_{dp})=\arg\left(\frac{P_l}{1-R_aR_b}\right),$$
$$\varphi_{refl}(\omega_{dp})=\arg\left(\frac{R_aP_r}{1-R_aR_b}\right). \tag{17}$$

The subscript nl refers to the nonlinear-overlap-region component and the subscript refl refers to the reflection-site component. Figure 1 illustrates the underlying conceptual two-source model that is predicted by the theoretical formalism. It is also interesting to consider the group delay of the resulting DPOAE

$$\tau_e(\omega_{dp}) \equiv -\frac{d\varphi_e}{d\omega_{dp}}, \tag{18}$$

The expected behavior of a_e, φ_e, and τ_e for fixed-ratio experiment can be illustrated by assuming that $\varphi_{nl} \approx$ constant, so that the entire phase variation with ω_{dp} arises through the change of φ_{refl} with ω_{dp}. Under this assumption, the variation of φ_{refl} can be related to the variation of $\arg(R_a)$ with ω_{dp} so that

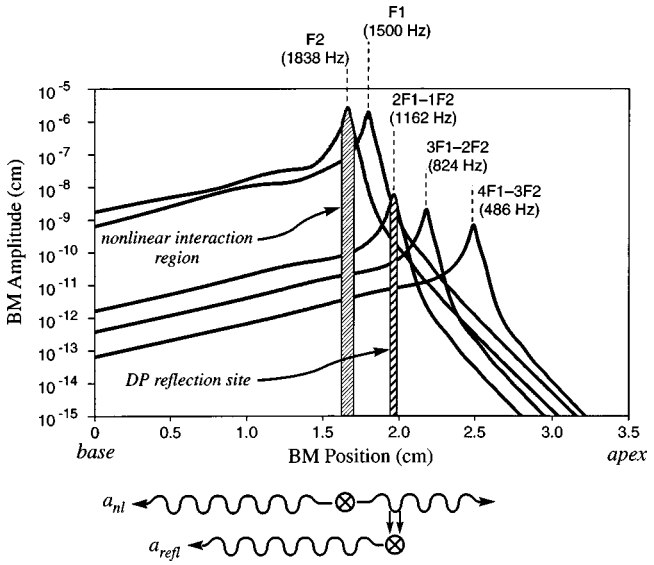

FIG. 1. Schematic diagram of the two-source model of DPOAE generation. Shown are the basilar membrane activity patterns of two primaries together with the resulting activity patterns of three apical DPOAEs generated by these primaries from a simulation using the model of Talmadge *et al.* (1998). The primaries interact in a region near the tonotopic place of the f_2 primary, so as to generate DP waves that travel both apically and basally. A fraction of the basally traveling DP wave is transmitted to the ear canal. The apically traveling DP wave propagates to the DP tonotopic place, where it is partially reflected basally, and is transmitted to the ear canal, where it interferes with the wave from the generation region. Not shown are multiple internal reflections of the two DP components, which in general will also be present.

$$\varphi_{\rm refl}(\omega_{\rm dp}) \cong \varphi_{\rm refl}(\omega_0) - \frac{\hat{k}(\omega_{\rm dp})}{k_\omega} \log\left(\frac{\omega_{\rm dp}}{\omega_0}\right). \tag{19}$$

Furthermore, the group delay τ_e can be related to the variation of $\varphi_{\rm refl}$ via:

$$\tau_e(\omega_{\rm dp}) \cong -\frac{d\varphi_e(\omega_{\rm dp})}{d\varphi_{\rm refl}(\omega_{\rm dp})} \frac{d\varphi_{\rm refl}(\omega_{\rm dp})}{d\omega_{\rm dp}}$$

$$= +\frac{\hat{k}}{2\pi\omega_{\rm dp}k_\omega} \frac{d\varphi_e(\omega_{\rm dp})}{d\varphi_{\rm refl}}. \tag{20}$$

In analyzing the predictions of the model under the assumption of $\varphi_{\rm nl} \approx$ constant, it is important to note that two cases are of importance, namely those for $a_{\rm nl} > a_{\rm refl}$ and $a_{\rm nl} < a_{\rm refl}$.

The resulting phasor diagrams of the interference between the two components are shown in Fig. 2(a), when $a_{\rm nl} > a_{\rm refl}$ (i.e., the overlap-region component is dominant). As is evident from this diagram, $-\pi < \varphi_e < +\pi$ as $\varphi_{\rm refl}$ is varied under these circumstances, with the most rapid phase variation of a_e and φ_e occurring when $\varphi_{\rm refl} \cong (2n+1/2)\pi$ $(n+0,\pm1,\pm2,...)$, as shown in Fig. 2(b). Also shown is the group delay τ_e, which has minima and maxima which positively correlate with the minima and maxima of a_e.

The phasor diagram of the two-component interference is shown in Fig. 2(c), for the case of $a_{\rm nl} < a_{\rm refl}$ (i.e., the reflection-site component is dominant). Under these circumstances, φ_e is unbounded, with the maximum variation of a_e and φ_e again occurring when $\varphi_{\rm refl} \cong (2n+1/2)\pi$, as shown in Fig. 2(d). Furthermore, τ_e now has minima and maxima which negatively correlate with the minima and maxima of a_e. Finally, it should be noted that the positive derivative of φ_e with respect to $\varphi_{\rm refl}$ will result in a negative slope of φ_e when plotted against $\omega_{\rm dp}$, as is evident from Eq. (19).

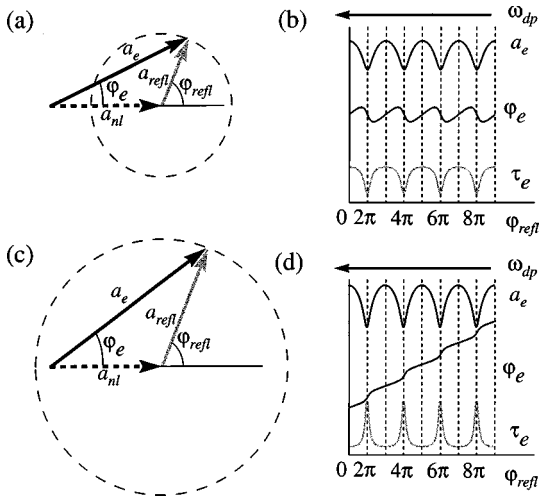

FIG. 2. Phasor diagrams and patterns of DPOAE amplitude (a_e), phase (ϕ_e) and group delay (τ_e) for the interference of two DP sources. Shown in (a) and (b) are the phasor diagram and resulting amplitude, phase, and group-delay behavior for the case $a_{\rm nl} > a_{\rm refl}$, where $a_{\rm nl}$ and $a_{\rm refl}$ are the DPOAE amplitudes corresponding, respectively, to the nonlinear generation region and to the reflection site. Similarly the phasor diagram and resulting amplitude, phase, and group-delay behavior are shown in (c) and (d), respectively, for the case $a_{\rm nl} < a_{\rm refl}$. Because an increasing $\varphi_{\rm refl}$ corresponds to a decreasing $\omega_{\rm dp}$ (as indicated by the arrows), a positive slope of φ_e when plotted against $\varphi_{\rm refl}$ corresponds to a negative slope when plotted against $\omega_{\rm dp}$.

Figure 2(b) and (d) show distinctive patterns of behavior for the DPOAE amplitude, phase, and group delay which are categorically different for the cases $a_{\rm nl} > a_{\rm refl}$ and $a_{\rm nl} < a_{\rm refl}$. Moreover, since the reflection-site component can be suppressed by an external tone near in frequency to the DPOAE (e.g., Kummer *et al.*, 1995; Gaskill and Brown, 1996; Heitmann *et al.*, 1997), this model implies that when the DPOAE amplitude, phase, and group delay follow that shown in Fig. 2(d), suppression by an external tone should shift the behavior to that shown in Fig. 2(b).

C. Application of model to pulsed-tone measurements

When one primary tone is pulsed and the other is on continuously, the DPOAEs generated by these tones will also be pulsed. Since the reflection-site component has a longer latency than the overlap-region component, this also means that during each DPOAE pulse, there will be a time interval (starting shortly after the turn-on of the primary tone) during which only the shorter-latency overlap-region component will be present, and an interval in which the longer-latency reflection-site component will dominate (starting shortly after the turn-off of the primary tone). Those situations are illustrated in Fig. 3, which shows the two components for the case (a) when $a_{\rm refl} > a_{\rm nl}$ (i.e., the reflection-site component is dominant), and case (b) when $a_{\rm refl} < a_{\rm nl}$ (i.e., the overlap site is dominant). In obtaining these plots, it was assumed that

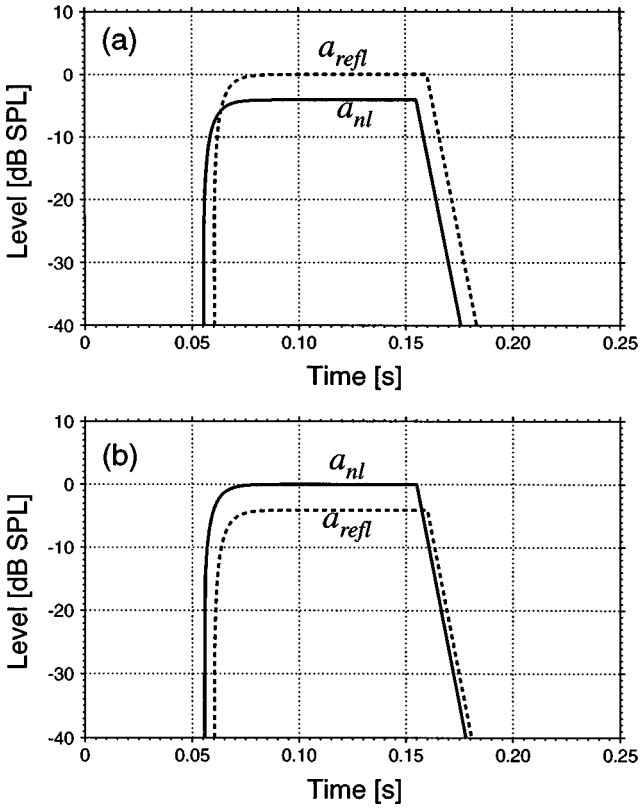

FIG. 3. The expected levels of the overlap-region component (solid line) and the reflection-site component (dashed line) for (a) the case $a_{\rm refl} > a_{\rm nl}$ and (b) the case when $a_{\rm refl} < a_{\rm nl}$. In both cases, the f_2 primary was assumed to be pulsed in the interval $0.05\ {\rm s} < t < 0.15\ {\rm s}$. The two DPOAE components were assumed to have exponential growth/decay behaviors, as described in the text [Eqs. (21) and (22)]. Note that the two lines intersect shortly after the turn-on of the external tone in (a) and shortly after the turn-off of the tone in (b).

each of the two components had exponential growth/decay behaviors, with the overlap-region component having a shorter latency than the reflection-site component. In more detail, the model used was

$$a_{\rm nl}(t) = \begin{cases} 0, & t < T_{\rm on} + \tilde{\tau}_{\rm n1} \\ a_{\rm nl}(1 - e^{-\gamma(t - T_{\rm on} - \tilde{\tau}_{\rm nl})}), & T_{\rm on} + \tilde{\tau}_{\rm n1} \leqslant t < T_{\rm off} + \tilde{\tau}_{\rm nl} \\ a_{\rm nl}\, e^{-\gamma(t -> T_{\rm off} - \tilde{\tau}_{\rm n1})}, & t \geqslant T_{\rm off} + \tilde{\tau}_{\rm nl}, \end{cases} \tag{21}$$

for the overlap-region component, and

$$a_{\rm refl}(t) = \begin{cases} 0, & t < T_{\rm on} + \tilde{\tau}_{\rm dp} \\ a_{\rm refl}(1 - e^{-\gamma(t - T_{\rm on} - \tilde{\tau}_{\rm dp})}), & T_{\rm on} + \tilde{\tau}_{\rm dp} \leqslant t < T_{\rm off} + \tilde{\tau}_{\rm dp} \\ a_{\rm refl} e^{-\gamma(t - T_{\rm off} - \tilde{\tau}_{\rm dp})}, & t \geqslant T_{\rm off} + \tilde{\tau}_{\rm dp}, \end{cases} \tag{22}$$

for the reflection-site component, where $\tilde{\tau}_{\rm dp} > \tilde{\tau}_{\rm nl}$. Here, $T_{\rm on}$ is the turn-on time of the f_2 external tone, and $T_{\rm off}$ is the turn-off time of the tone.

The parameters $\tilde{\tau}_{\rm nl}$ and $\tilde{\tau}_{\rm dp}$ can be shown to have simple forms in terms of the underlying travel times of the transpartition pressure waves for frequencies ω_2 and $\omega_{\rm dp}$. In terms of $\tau(x,\omega)$, the travel time of a pressure wave of frequency ω from the base to a location x on the basilar membrane, $\tilde{\tau}_{\rm nl}$ and $\tilde{\tau}_{\rm dp}$ may be expressed as

$$\tilde{\tau}_{\rm nl} = \hat{\tau}_2 + \tau(\hat{x}_2, \omega_{\rm dp}), \tag{23}$$

$$\tilde{\tau}_{\rm dp} = \hat{\tau}_2 + 2\hat{\tau}_{\rm dp} - \tau(\hat{x}_2, \omega_{\rm dp}), \tag{24}$$

where $\hat{\tau}_2 \equiv \tau(\hat{x}_2, \omega_2)$ and $\hat{\tau}_{\rm dp} = \tau(\hat{x}_{\rm dp}, \omega_{\rm dp})$. It should be noted that $\tau(\hat{x}_2, \omega_{\rm dp})$ is very small compared to either $\hat{\tau}_2$ or $\hat{\tau}_{\rm dp}$, for large ratios of ω_2/ω_1 (i.e., $\omega_2/\omega_1 \gtrsim 1.1$). This is a consequence of the fact that the reverse traveling wave from the tonotopic place $x = \hat{x}_2$ to the cochlear base ($x = 0$) occurs entirely in the long-wave region of the DP traveling wave.

In addition to the two components shown in Fig. 3, there will be DP components arising from multiple internal reflection of these two components. These can be obtained by expanding Eq. (1) with respect to $R_a R_b$. If

$$R_a(\omega_{\rm dp}) \cong |R_a(\omega_{\rm dp})| e^{i\phi_a - 2i\omega_{\rm dp}\tau_{\rm dp}}, \tag{25}$$

$$R_b(\omega_{\rm dp}) \cong |R_b(\omega_{\rm dp})| e^{i\phi_b - i\omega_{\rm dp}\tau_b}, \tag{26}$$

then

$$\begin{aligned} P_e(\omega_{\rm dp}, t) &= a_e(t)\cos[\omega_{\rm dp} t + \varphi_e(t)] \\ &= a_{\rm nl}(t)\cos(\omega_{\rm dp} t + \phi_{\rm nl}) + a_{\rm refl}(t)\cos(\omega_{\rm dp} + \phi_{\rm dp}) \\ &\quad + |R_a(\omega_{\rm dp}) R_b(\omega_{\rm dp})| a_{\rm nl}(t - 2\hat{\tau}_{\rm dp} - \hat{\tau}_b) \\ &\quad \times \cos[\omega_{\rm dp}(t - 2\hat{\tau}_{\rm dp} - \hat{\tau}_b) + \varphi_{\rm nl} + \phi_a + \phi_b] \\ &\quad + |R_a(\omega_{\rm dp}) R_b(\omega_{\rm dp})| a_{\rm refl}(t - 2\hat{\tau}_{\rm dp} - \hat{\tau}_b) \\ &\quad \times \cos[\omega_{\rm dp}(t - 2\hat{\tau}_{\rm dp} - \hat{\tau}_b) + \varphi_{\rm refl} + \phi_a + \phi_b] \\ &\quad + \cdots . \end{aligned} \tag{27}$$

Equation (25) was obtained by noting that $d\varphi_a/d\omega_{\rm dp} \cong -2\hat{\tau}_{\rm dp}$ (e.g., Talmadge *et al.*, 1998). A detailed derivation of a generalization of Eq. (27), for several types of simplifying assumptions about Eq. (1), will be presented in a future publication.

The predicted DPOAE amplitude and phase behavior from this model are shown in Fig. 4. From this figure, the experimental DPOAE phenomenology is expected to be fairly complex for the two-source model, in part because of the presence of two time-delayed (with different delay amounts) components, plus multiple internal reflections of these components. In Fig. 4, only the case where the overlap-region and reflection-site components destructively interfere is considered. In addition, the phase shifts of each of the multiple internal reflections were also chosen to give destructive interference. Models which do not have significant internal reflection would not give rise to multiple-delay DPOAE components, and are expected to have a much simpler phenomenology as a result.

The presence of the nulls in Fig. 4 can be understood by noting the location of the intersection of the curves for the two components in Fig. 3(a) and (b), which in the case of destructive interference would correspond to the location of minima (''nulls'') in the DPOAE amplitude. The case for $a_{\rm refl} > a_{\rm nl}$ is represented in Fig. 3(a). The two curves intersect shortly after the f_2 primary is turned on. This behavior indi-

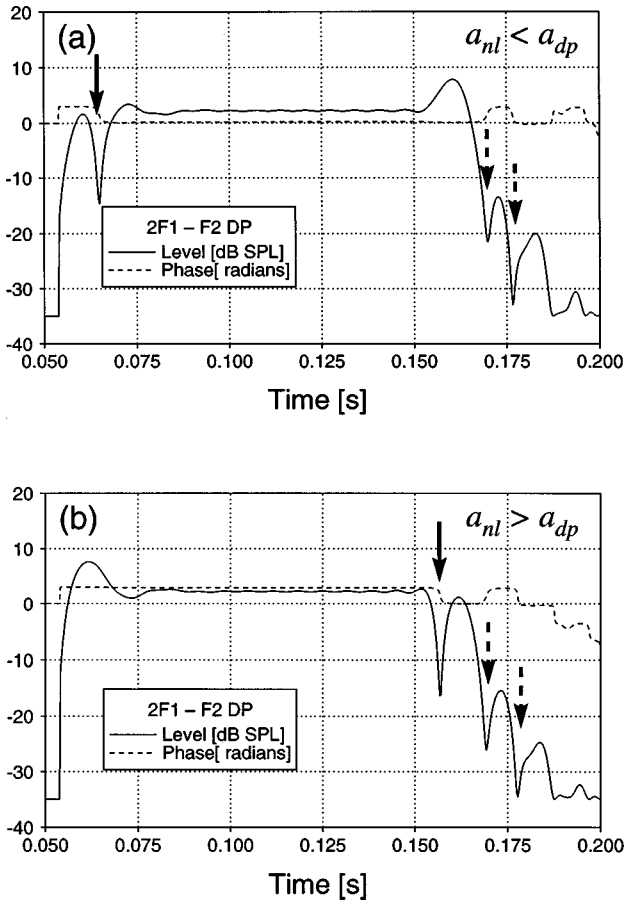

FIG. 4. Predicted DPOAE amplitude and phase, when the phases of the overlap-region and reflection-site components are 180 deg out of phase for the cases (a) when the component from the reflection site is 6 dB larger than that from the overlap site, and (b) when the reflection-site component is 6 dB smaller than the component from the overlap site. The f_2 primary was assumed to be pulsed in the interval $0.05\ \text{s} < t < 0.15\ \text{s}$. The DPOAE signal was filtered by a 300-Hz-wide bandpass filter and a -35 dB SPL additive noise floor was included in order to simulate realistic experimental conditions. For both cases, the phase difference between the overlap and the reflection-site components and the phase shift from multiple internal was -3.0 rad. Notice the presence of a null [see the solid arrow in (a)] in DPOAE amplitude and a corresponding step in DPOAE phase shortly after the turn-on of the f_2 tone for case (a), which is shifted [see the solid arrow in (b)] to a position which is shortly after the turn-off of the f_2 tone for case (b). The interference notches after turn-off of the external tones that are present in both cases are due to destructive interference between successive multiply reflected components, and is a result of the -3.0 rad choice of phase shift per multiple reflection.

cates the presence of an interference null shortly after signal turn-on. For the case $a_{\text{refl}} < a_{\text{nl}}$ illustrated in Fig. 3(b), the curve for the reflection-site component is shifted downward relative to the curve for the overlap-region component, which in turn shifts the intersection of the two curves (and the associated null in DPOAE amplitude) shortly after the f_2 primary is turned off.

II. GENERAL METHODS

A. Subjects

The four subjects used in this study were volunteers from the Purdue University community and varied in age from 20 to 54 years. The subjects were selected after intensive screening procedures, which included multifrequency tympanometry, audiometric thresholds, audiologic history, and the evaluation of spontaneous, transient-evoked and distortion product otoacoustic emissions. The subjects were selected from a larger group on the basis of the pattern of DPOAEs seen in their ears.

B. Data collection

Data were collected with the subject seated in a recliner chair inside a double-walled IAC sound-treated booth. In order to reduce the variability in the measurements, no recordings were obtained until approximately 15 min after the subject was seated in the booth. An Etymotic ER10 low-noise microphone assembly was coupled to the ear by the appropriately sized GSI tip. The signal was amplified by the preamplifier supplied by Etymotic, and then filtered (300–10000 Hz, roll off=6 dB/octave, gain=200) by a battery-run Stanford SR-560 low-noise amplifier under control of a NeXT computer. The signal from the SR-560 amplifier was connected to a Singular Solutions 64x A/D converter via balanced microphone cables. The A/D 64x generated 16-bit samples at a sampling rate of 44.1 kHz. The signal was 64 times over-sampled and converted using a bit-stream A/D converter. A customized program was used to control the presentation of the stimuli and recording of responses. The data were reduced by averaging successive segments (usually 44 100 samples—1 s) before being saved to disk to be analyzed off-line.

Acoustic signals were digitally generated using the floating point coprocessor of the NeXTstation computer with software written in our laboratory. It was then converted to analog signals via the NeXTstation's on-board 16-bit D/A converters at 44 100 Hz. The system clock on the NeXTstation is not identical with the clock on the A/D 64x. The clock on the computer was continually monitored by recording a stimulus from the NeXT computer and determining the frequency using the A/D 64x. The output frequencies were modified to compensate for the differences in the clocks. The acoustic signals were then passed through TDT attenuators, whose levels were controlled through a serial line by the NeXTstation, before being passed through TDT microphone buffers to two Etymotic ER-2 tube-phone assemblies coupled to the ER10 microphones. Most of the studies were done with just the two primaries, which were generated in separate channels and controlled by separate attenuators. A third tone was needed in DPOAE fine-structure suppression experiments (e.g., Kemp and Brown, 1983; Heitmann *et al.*, 1998). In these experiments, the two furthest-separated tones (the suppressor tone and f_2) were generated in one channel, and presented through the same ER2.

The stimulus-delivery setup was calibrated using a Zwislocki coupler. Since the ER-2 transducer is designed to produce a flat response in a Zwislocki coupler (DB-100) when properly coupled to an ER-10 probe, the frequency response of the ER-2 transducer when used with the ER-10 probe would be nearly flat at the eardrum in the average human ear. For these reasons we used the iso-voltage stimulus-presentation strategy, in which the voltage presented to transducers is held constant over frequency. The iso-voltage strategy is not subject to the large, idiosyncratic

increases of eardrum stimulus SPL between 3.5 and 7 kHz that are produced by the alternate in-the-ear adjustment strategy (Siegel and Hirohata, 1994; Whitehead *et al.*, 1995). Variations in geometry of individual ear canals and eardrum impedances can, however, produce differences between the SPL produced in an ear by the ER-2 and that in a Zwislocki coupler, which was not designed to accurately simulate real ears above 4 kHz. These departures are not relevant for the frequencies used here and are smaller than the discrepancies produced by calibrating at the position of the probe.

Custom-built programs were used to generate and control the stimuli, record the data, and control the durations, levels, and frequencies of the stimuli, which were presented in random order. The progress of the experiment was monitored using the computer display, which indicated which stimuli were being presented and the peak levels of the data throughout the experiment. Additional monitoring was done by fast Fourier-transform (FFT) analysis of completed data files on additional NeXT computers in the laboratory, which were networked with the data-collection computer.

C. Data Analysis

All data analysis was done off-line. Since the frequencies of the distortion products have a known relationship to those of the primaries, the data can be fit to a model of the expected frequencies of the known signal components. A least-squares fit (LSF) analysis (see Long and Talmadge, 1997) is then performed on the averaged data to determine the levels and phases of these components. The LSF analysis uses a series of basic sinusoidal functions of known frequencies in order to fit a particular signal. It has the advantage that any known frequency component can be distinguished and measured, even if it does not fall within one bin of the FFT. Such resolution would be otherwise impossible to achieve with a standard FFT algorithm. It also allows for the separation of a small signal from the spectral splatter of a neighboring larger one, which would inherently add the energy (aliasing effect) in the common frequency bin of the usual FFT and elevate the measured level. Another advantage of the LSF technique is the overall reduction in required CPU time. While the FFT algorithm performs $N \log N$ operations to evaluate N frequency components per window of length N, the LSF filter performs only $k \cdot N$ operations, for k discrete frequency components inside a spectral window of width N (Long and Talmadge, 1997). This technique removes correlations between adjacent frequency components. It therefore provides a significant improvement in frequency resolution over the conventional FFT by permitting the elimination of spectral splatter at the cost of a poorer signal-to-noise ratio when the DPOAE is close to a stimulus component. FFT analysis was done on a subset of the data in order to establish that the LSF paradigm gives equivalent data.

III. STUDY 1: CONTINUOUS PRIMARIES

The root source of distortion in the model is the nonlinear interaction of the traveling waves of the two primaries on the basilar membrane. Maximal interaction occurs in the overlap region around the f_2 place. The generated waves with acoustic energy at the DPOAE frequency propagates in both directions—basally towards the oval window and apically towards the DP tonotopic place (see Fig. 1). The DP wave transmitted apically from the generator region is partially reflected when it gets to the DP place, due to very small irregularities on the cochlear partition in conjunction with a tall/broad activity pattern (for details, see Talmadge *et al.*, 1998). The ''place-fixed'' nature of the reflection mechanism will result in a rapid variation of the phase of the reflectance with DP frequency. On the other hand, the phase of the DPOAE component from the overlap region, for the fixed f_2/f_1 paradigm, will be only weakly dependent on the DP frequency from the approximate scale invariance of the cochlea. DPOAEs are the result of the summation of these two waves (plus any subsequent cochlear waves basally incident on the oval window stemming from multiple basal/apical reflections of the DP waves in the cochlea). The different rates of phase change of the two components produce the interference pattern known as DPOAE fine structure. This interference pattern is not completely regular because the amplitude and phase of the reflection-site component depends on the nature of the cochlear irregularities and cochlear filtering (see Talmadge *et al.*, 1998).

A comparison of the amplitude and phase behavior of DPOAE from fixed-ratio experiments permits evaluation of the relative amplitudes of the components from two sources. If a small component a_{refl} with rapidly changing phase is added to a larger one a_{nl} which is slowly changing in phase ($a_{\mathrm{nl}} > a_{\mathrm{refl}}$), the resulting phase will fluctuate around the slowly varying one of the generation-region component and have a rounded, sawtoothed appearance [see Fig. 2(b)]. In contrast, if a large component with rapidly changing phase is added to a small component with slowly changing phase ($a_{\mathrm{refl}} > a_{\mathrm{nl}}$), the resulting phase will change more rapidly in a ramp-like fashion near the DPOAE minima [see Fig. 2(d)]. Since group delay is the derivative of phase, DPOAE group delay will be positively correlated with amplitude fine structure when $a_{\mathrm{nl}} > a_{\mathrm{refl}}$, and negatively correlated with the amplitude fine structure when $a_{\mathrm{refl}} > a_{\mathrm{nl}}$ (see Fig. 2).

A. Methods

The ratio of continuous primaries was kept constant as the frequencies of the primaries were varied so as to sweep the frequency of the DPOAE through a range of values. The recording of the ear-canal signal was triggered to start at signal onset when the two primaries had zero phase. Four s of data were reduced to 1 s by averaging, and then stored to disk to be analyzed later using a least-squares fit analysis (see below) to obtain the amplitudes, phases, and noise floors of the two primaries and a number of their cubic distortion products ($f_{\mathrm{dp}}^{n} = nf_1 + n(f_2 - f_1)$; $n = -3, -2, -1, 0, 1, 2, 3, 4$). The frequency ratio of the primaries for these measurements was $f_2/f_1 = 1.225$ and the levels were $L_1 = 65$ dB and $L_2 = 50$, 55, 60, or 65 dB SPL). These measurement conditions are optimal for generating the $2f_1 - f_2$ distortion product, which is the only one considered in this paper.

An algorithm based on summation and subtraction of overlapping data segments (whose lengths were an integral

number of periods associated with the frequencies of the stimuli and of the DPOAEs) was used to estimate the level of the DPOAE and the level of the noise floor for each DPOAE. This algorithm reduces the noise floor through the performance of additional averages, and provides an estimate of the noise floor at the frequency of each DPOAE (cf. Stover *et al.*, 1996). The subtraction cancels out the DPOAE components of the signal but leaves noise components which are not correlated with the signal. Depending on the sample length used for the least-squares-fit estimate (7350 or 11 020 samples), several estimates of the level of the DPOAE were obtained from each pair of primaries. The medians of these estimates were calculated and used as the estimate of the DPOAE level.

The group delay was obtained by performing a least-squares fit to a straight line in consecutive 10-point intervals of the DPOAE phase. The group delay for this algorithm was just $-m_\varphi/2\pi$, where m_φ is the slope of the straight line. This algorithm produced estimates for the group delay which were far less noisy than those obtained with other alternatives, such as numerical differentiation of the DPOAE phase.

1. Experimental protocol

A prospective subject was first screened using the fixed-ratio paradigm with a relatively coarse frequency step-size. The step-size varied with DPOAE frequency and was chosen to correspond to separations in DPOAE tonotopic position along the basilar membrane of 0.05 mm, based on the Greenwood place–frequency map (Greenwood, 1990). For frequencies in the range 1500–2000 Hz, this tonotopic spacing corresponded to frequency spacings of 18–24 Hz. Since the tonotopic separation between adjacent DPOAE amplitude maxima corresponds to approximately 0.4 mm (e.g., Talmadge *et al.*, 1993), the granularity of the DPOAE measurements resulted in approximately eight DPOAE values per fine-structure period.

Subjects were selected for further testing using the criteria that the $2f_1-f_2$ DPOAEs were high enough in level to give at least a 40-dB signal-to-noise ratio at the fine-structure maxima, and that the amplitude variations of the fine structure were at least 10 dB. In some cases, a selection was also made on the basis that the amplitude and group delay fine structures were anticorrelated (e.g., Talmadge *et al.*, 1998). These criteria assured that the main predictions of the two-source model could easily be tested in follow-up measurements.

Detailed fine-structure measurements on selected subjects were made using the fixed-ratio paradigm. For each subject, one or more fine-structure regions extending between two adjacent maxima was chosen for further investigation. Fine structures were selected so as to provide examples of the situations in which the generation-region DPOAE was dominant [see Fig. 2(a), (b); rounded saw-tooth phase behavior] or the DP-place component was dominant [see Fig. 2(c), (d); ramp-like phase behavior]. For each fine structure investigated, the DPOAE frequencies were selected so that they covered a frequency region containing two adjacent DPOAE amplitude maxima, and the frequencies of the primaries were selected to provide DPOAE estimates every 6 Hz, except near deep-amplitude minima, where the frequency spacing was reduced to 2 Hz.

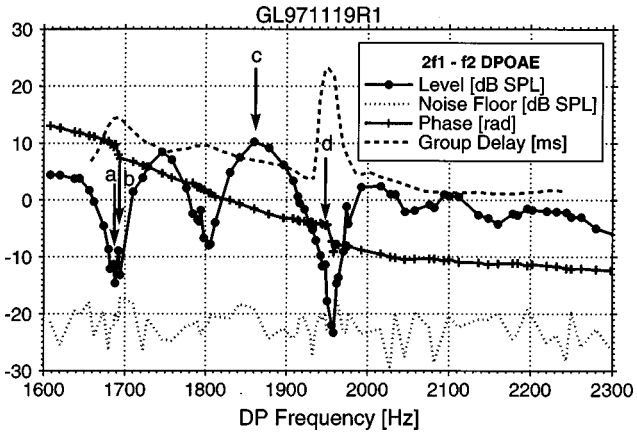

FIG. 5. $2f_1-f_2$ DPOAE level, phase, and group delay as a function of the DPOAE frequency for subject GL, where $f_2/f_1=1.225$, $L_1=65$ dB SPL, and $L_2=55$ dB SPL. The arrows indicate the frequencies for which pulsed-tone measurements are plotted in Fig. 8.

B. Results

The amplitude, phase, and group delay of DPOAEs are presented for three of the six subjects in Figs. 5, 6, and 7. Close examination of Figs. 5, 6, and 7 reveals that whenever there was a minimum in the DPOAE fine structure, there was also a change in the overall trend of a slowly decreasing phase with increasing frequency. The rate of departure from this background phase depended on the depth of the amplitude minimum (note the different frequency scales for the different subjects). The phase transition was either a steep, localized slope in phase giving a ramp-like appearance (see Fig. 5) or a temporary increase in phase providing a saw-toothed appearance (see Figs. 6 and 7). The change in the phase was maximal at the amplitude minimum. The extracted group delay was negatively correlated with DPOAE level for subject GL [compare with Fig. 2(d)] and positively correlated for subjects NZ and AB [compare with Fig. 2(b)].

When the two components were nearly equal in level (deep fine structure), the phase changed rapidly and very fine resolution was needed to distinguish between the two phase behaviors. The problem was exacerbated by the (expected) poor signal-to-noise ratio near these minima. Frequency sweeps with improved frequency resolution serve to better define the phase transition. Note the increased proximity of the points near fine structure minima in Figs. 5, 6, and 7). This reflects the additional data from the fine-resolution sweeps. Examples of the fine-resolution sweeps on a more expanded scale can be seen in Figs. 11 and 12. When the two components were nearly equal in level (deep fine structure), the pattern could vary on different days or with different recording conditions. An example of this may be seen by comparing the the sharp minimum near 1950 Hz, which is shown in Figs. 5 and 11. Similarly, compare the minimum near 1200 Hz in Figs. 7 and 13. For this reason, a complete set of measurements were obtained in a single session (preferably without removing the probe from the ear) whenever possible.

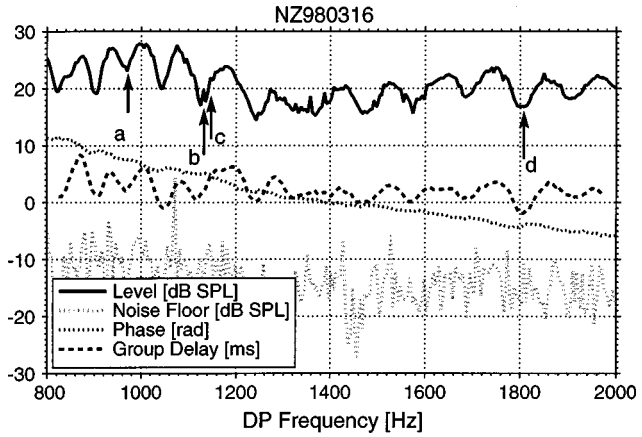

FIG. 6. $2f_1-f_2$ DPOAE level, phase, and group delay as a function of the DPOAE frequency for subject NZ, where $f_2/f_1=1.225$, $L_1=65$ dB SPL, and $L_2=50$ dB SPL. The arrows indicate the frequencies for which pulsed-tone measurements are plotted in Fig. 9. Too many data points were collected to permit the use of symbols to differentiate the different sets of data. Line styles are used instead.

C. Discussion

The two patterns seen in the mathematical model (see Fig. 2) can also be seen in the data (see Figs. 5, 6, and 7). In Fig. 5, the DPOAE amplitude minima around 1690, 1800, and 1950 Hz, and the associated phase and group delays correspond to the case of $a_{\text{refl}}>a_{\text{nl}}$ in Fig. 2(c) and (d). In Figs. 6 and 7, the amplitude minima correlate with the group delay minima, as expected for the case $a_{\text{refl}}<a_{\text{nl}}$ in Fig. 2(a) and (b). Although the data presented in this paper show a consistent pattern in a given subject, this is not always the case. It is possible for two adjacent minima to differ in the sense that for one, $a_{\text{nl}}>a_{\text{refl}}$, while for the other, $a_{\text{refl}}>a_{\text{nl}}$. When the two components are very nearly equal in level, so that there is a deep DPOAE minimum due to nearly complete cancellation, small changes in the components from session to session could cause a large change in the DPOAE level. Changes in cochlear function, in the properties of the middle ear, or in the impedance or location of the probe assembly in the ear canal could produce these small changes in the source amplitudes.

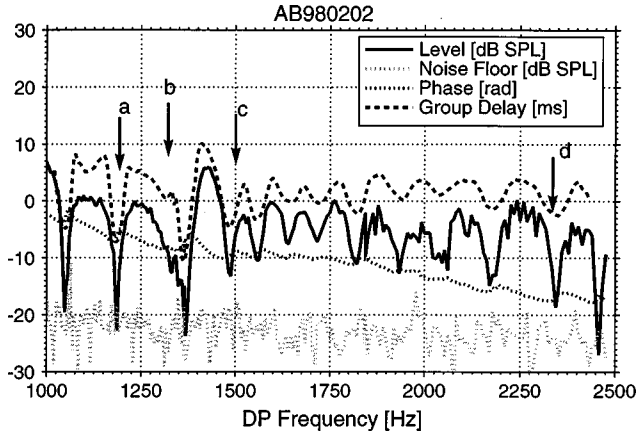

FIG. 7. $2f_1-f_2$ DPOAE level, phase, and group delay as a function of the DPOAE frequency for subject AB, where $f_2/f_1=1.225$, $L_1=65$ dB SPL, and $L_2=50$ dB SPL. The arrows indicate the frequencies for which pulsed-tone measurements are plotted in Fig. 10.

IV. STUDY 2: PULSED PRIMARY

The DPOAE components are expected to have different latencies. The latency of a_{nl} will be only slightly longer than the time for propagation of the f_2 wave from the cochlear base to the f_2 tonotopic place [see Eq. (23)]. This travel time is the main determinant of the latency of the generator-site component of the DPOAE. This is because the travel time for propagation of a DP wave from the f_2 tonotopic site to the cochlear base will be very short, since the travel occurs in the long-wave region of the DP traveling wave. The associated phase will vary weakly with DP frequency, and consequently the phase derivative (related to group delay) will also be small. The latency of a_{refl} is approximately the latency of a_{nl} plus twice the travel time for a DP wave to propagate from the f_2 tonotopic site to the DP place [see Eq. (24)]. Consequently, a second way of separating these components is to examine the level and phase at DPOAE turn-on and turn-off.

Whitehead *et al.* (1996) provided some support for two sources of DPOAEs by showing that the phase of the DPOAE could change soon after its onset. This was confirmed for the $2f_1-f_2$ DPOAE by Martin *et al.* (1998). A modification of the procedure used by Whitehead *et al.* permits the study of the growth and decay of the DPOAE when the level of the higher-frequency primary was modulated in level. Our models make it clear that, although other characteristics of pulsed DPOAE provide information about the relative levels of the components, there is one feature that clearly identifies which of the two components is greater in magnitude.

If a pulsed DPOAE paradigm measurement is performed at a DP frequency near a fine-structure minimum (where the two components are approximately out of phase), there will always be a clear notch either shortly after f_2 signal turn-on for $a_{\text{refl}}>a_{\text{nl}}$, or shortly after f_2 signal turn-off for $a_{\text{refl}}<a_{\text{nl}}$ (see Fig. 4). The notch is the result of destructive interference between the two components and occurs when the two components are very nearly equal in level. The location of the notch is represented in Fig. 3 by the intersection point of the a_{nl} and a_{refl} curves. As can be seen from this figure, there is exactly one intersection point of the two curves, which occurs either shortly after f_2 signal turn-on ($a_{\text{refl}}>a_{\text{nl}}$), or shortly after f_2 signal turn-off ($a_{\text{refl}}<a_{\text{nl}}$).

If all of the DP waves basally incident on the oval window were transmitted through the middle ear to the ear canal, one would have a summation of just the two components previously described. Since there is not, in general, a perfect impedance match, the incident DP waves at the oval window will be partially reflected back into the cochlea, and consequently re-reflected from the DPOAE site for the same reasons that the original apically traveling wave was reflected. This component will not be seen unless there is some reflection from the DP place. The re-reflected component will also sum with the original two sources, and some portion of these re-reflected waves will be reflected from the oval window to travel back to the DP place and be again reflected back towards the base of the cochlea, and so on. Consequently, even though there are only two cochlear sources, the additional reflections can produce a relatively complex temporal wave

form, as is seen in Fig. 4, if successive reflections are out of phase. The additional components occurring after stimulus turn-off are indicated by the dashed arrows. These additional reflections may also produce ripples after stimulus turn-on. If the successive multiple internally reflected components are in phase, a long tail in the decay of the DPOAE pulse will be observed instead.

A. Methods

For the pulsed primary tone (''pulsed-tone'') measurements, the f_2 primary was pulsed for 100 ms every 250 ms. The stimuli were presented for 16 s. The phases of the primaries were both 0 deg at the beginning of each signal, with the beginning of the first f_2 pulse occurring 50 ms into the signal. The turn-on and turn-off of the f_2 pulse was achieved using a rise/fall function with a 1-ms rise/fall time. In order to obtain partial cancellation of the primaries after averaging, the phase of the f_1 primary was rotated by 90 deg and the f_2 primary by 180 deg every 250 ms (e.g., Whitehead *et al.*, 1996). This choice of phase rotations left the $2f_1-1f_2$ DPOAE phase invariant under each rotation. The recording program was triggered to start recording the ear-canal signal at the start of the signal, and data was streamed to disk. When all of the four consecutive 250-ms segments of this signal are averaged together, the primary signals should cancel. Normally, about 55 dB of cancellation was achieved. The primaries did not cancel exactly due to clock-rate mismatches between the clocks for the D/A and the A/D, and because the frequencies of the clocks drifted slightly over the duration of a measurement (the total variation in the clock rates was about 0.02 Hz per h).

The phase rotation was achieved for most measurements by requiring that the frequencies of f_1 and f_2 be multiples of 4 Hz (to prevent an undesirable shift in the phases of the primaries between each 250-ms interval), and then rotating the phase of each primary using the signal-generation software. The disadvantage of this method was that an audible click was sometimes generated by the necessary change in the phase of the f_1 stimulus. Any transient evoked otoacoustic emission evoked by this click would have been minimal at the time of the onset of the f_2 pulse, which occurred 50 ms later. An alternative technique, which was used in some experiments, was to require that frequency f_1 be an odd number and f_2 be an even number not divisible by 4. In this way, no phase variation was required by the signal-generation software, since the phase offset of the f_1 primary was different by 90 deg and that of the f_2 primary by 180 deg every 250 ms. No clicks were detected with this method. There was no significant difference in the DPOAE responses obtained with the two methods.

The recorded data were averaged in 1-s nonoverlapping intervals (containing 4 250-ms pulses). Noisy data segments were identified and rejected by first histogramming the peak values in each 1-s interval. This histogram had a Gaussian-like distribution of peak values, and in some cases a small number of peak values which were much greater in value than the maximum of the Gaussian-like distribution. The 1-s average of the recorded data was made with the exclusion of the noisy data segments identified in this way.

Each 1-s average was then further averaged using 250-ms nonoverlapping intervals. Because of the phase rotation of the primaries between consecutive 250-ms intervals, this resulted in a signal dominated by the DPOAE of interest ($2f_1-f_2$ in this experiment) together with the remaining noise. Because of the nonexact cancellation of the primaries described above, a small residual signal at the f_1 and f_2 frequencies was usually also present.

A least-squares-fit filter with a window size of 150 points (giving a filter width of 300 Hz) was constructed and used to analyze the frequency components, $4f_1-3f_2$, $3f_1-2f_2,\ldots,4f_2-3f_1$. This filter was applied to the 250-ms averaged data using a 50-point offset between consecutive applications of the filter.

1. Experimental protocol

As discussed in the Introduction and Sec. I, the two-source DPOAE model of Talmadge *et al.* (1997, 1998) makes definitive, testable predictions for the relationship between the DPOAE amplitude and phase for both fixed-ratio and pulsed-tone measurements. In order to test the self-consistency of these predictions, it was necessary that both sets of measurements be performed as close together in time as possible. Part of the reason for this is that removal and reinsertion of the microphone assembly in the ear canal could produce potentially confounding effects. Additionally, it was noted during the measurements that some shifts in the levels and phases of the DPOAEs occurred from day to day. Consequently, care was taken to perform pulsed and continuous primary measurements in the same experimental session whenever possible. Selected DPOAE frequencies from the detailed sweeps in experiment 1 were chosen for the pulsed-tone measurements. Experiments under a given set of conditions were typically repeated 16–32 times to improve the signal-to-noise ratio.

B. Results

The changes in the levels and phases of DPOAEs at the turn-on and turn-off of f_2 pulses were evaluated for the conditions indicated by the lettered arrows in Figs. 5, 6, and 7. When the DPOAE frequency was near that of a fine-structure amplitude maximum (so that the signals from the two sources were in phase), it was not easy to separate the two components [e.g., Fig. 8(c)]. When the DPOAE frequency was near that for a deep fine-structure minimum (corresponding to an approximately 180 deg phase difference or destructive interference), the DPOAE level was largest at the turn-on and turn-off of the DPOAE pulse (when only one component was present). The signal-to-noise ratio is poor for the remainder of the pulse when the two components are present [see Fig. 8(d)]. The measured phase in the two bursts regions was consistent with that giving destructive interference.

The most interesting patterns are those obtained on the steep slopes surrounding a fine-structure amplitude minimum when the components were partially canceled (see Figs. 8, 9, and 10). The signal-to-noise was much better for this choice

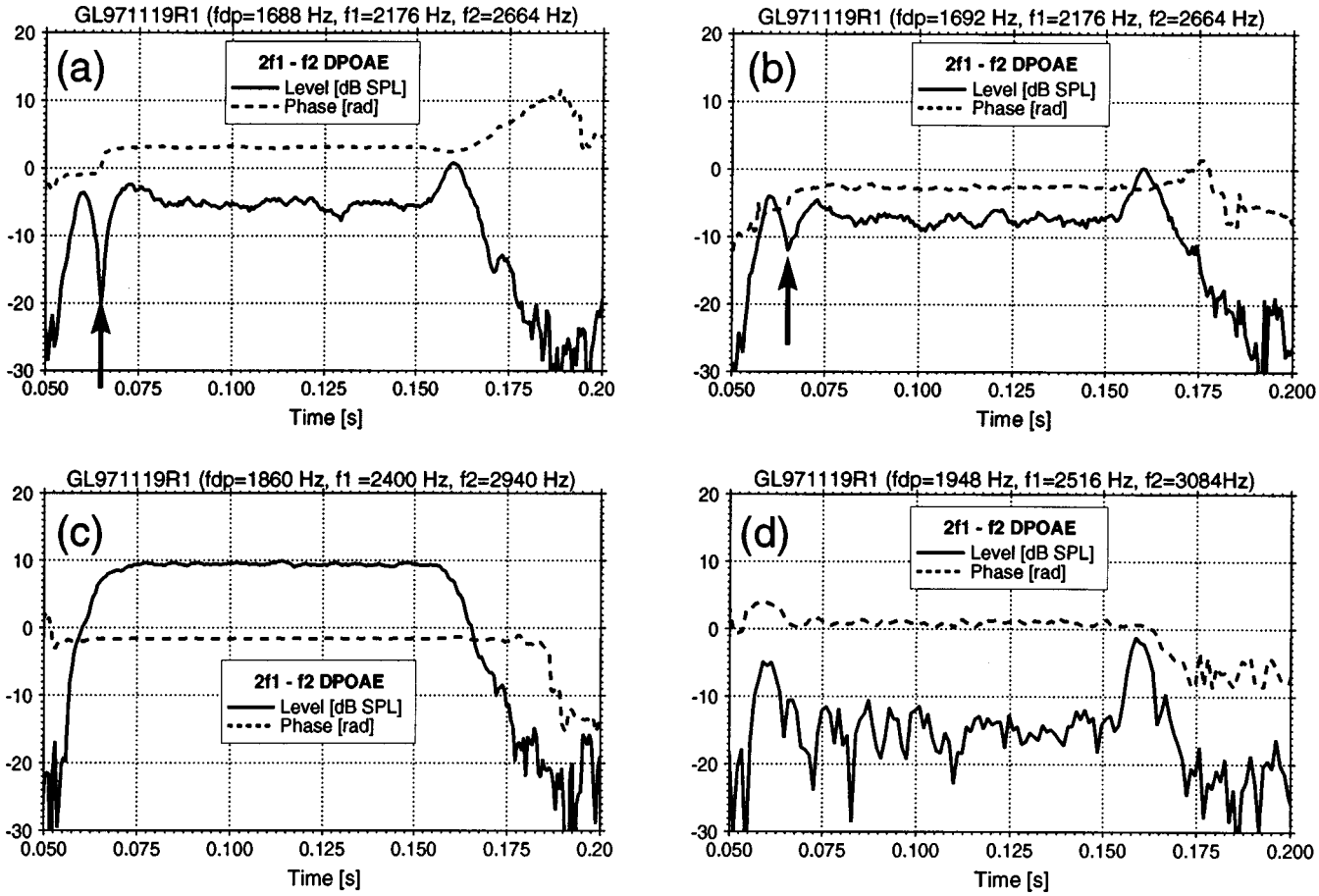

FIG. 8. 2 f_1-f_2 DPOAE level and phase as a function of time for subject GL for various choices of f_{dp} when f_2 is pulsed on from 50 ms to 150 ms. The frequency ratio and levels of the primaries are the same as in Fig. 5. The arrows in this figure point to the interference notch discussed in Sec. IV C and indicated in Fig. 4.

(typically>10 dB) and it produced the clearest representations of the (destructive) interference of the two DPOAE components. The responses to the pulsed f_2 tone from GL [Fig. 8(a) and (b)] had a downward notch after stimulus onset, and the data from the other two subjects NZ and AB (Figs. 9 and 10) had a similar notch after stimulus turn-off. The notches are indicated by arrows. Whenever there was a notch in the amplitude function, there was a rapid change in the phase of the DPOAE. Note that not only the notches near stimulus turn-on and turn-off (indicated by the arrows) can be detected, but additional lobes with predictable amplitude and phase transitions can clearly be seen after stimulus turn-off. There are also regular ripples in the DPOAE amplitude after the notch at DPOAE onset [e.g., Fig. 9(b), (c)].

C. Discussion

When the continuous-tone phase behavior was ramp-like and thus indicated that $a_{\text{refl}}>a_{\text{nl}}$, the pulsed DPOAE data [see Figs. 8(a), (b)] was very similar to the model data for these conditions in Fig. 4(a). When the phase behavior for the continuous tones indicated that $a_{\text{nl}}>a_{\text{refl}}$, the pulsed DPOAE data [see Figs. 9, 10, and 15(b)] were similar to the model data for the same conditions [see Fig. 4(b)]. A step-like change in phase at the position of the notch can be used to aid in identification of the notch in noisy data such as Fig. 8(c). In addition to the notches after stimulus turn-on or turn-off, one can also see the expected pattern of additional lobes due to multiple reflections from the oval window and the DP site seen in Fig. 4.

Since the initial response is always from the generation region, and the response after stimulus turn-off is primarily from the reflection component, it might be thought that the initial and final DPOAE bursts could be used as an indicator of relative amplitudes of the two DPOAE components. Although the relative amplitudes of these two bursts were always consistent with the position of the notch, these indicators may not be reliable. The initial burst may not have time to reach its final amplitude before the onset of the component from the DP site starts to reduce the DPOAE level, reflections from the oval window may modify the level of the response after signal turn-off and efferent stimulation (cf. Liberman *et al.*, 1996), or fatigue may also modify the DPOAE level from the beginning to the end of the pulse.

The DPOAE amplitude fine structure of a given subject was observed to vary from session to session, and even over the course of a single session. This variability is suggestive of that for the variation of spontaneous otoacoustic emissions previously reported by Whitehead (1991). As was the case with Whitehead's observations, the most significant variation within a session usually came during the first 30 min after the subject was placed in the recording booth. (As was discussed in the Methods section, no measurements were taken

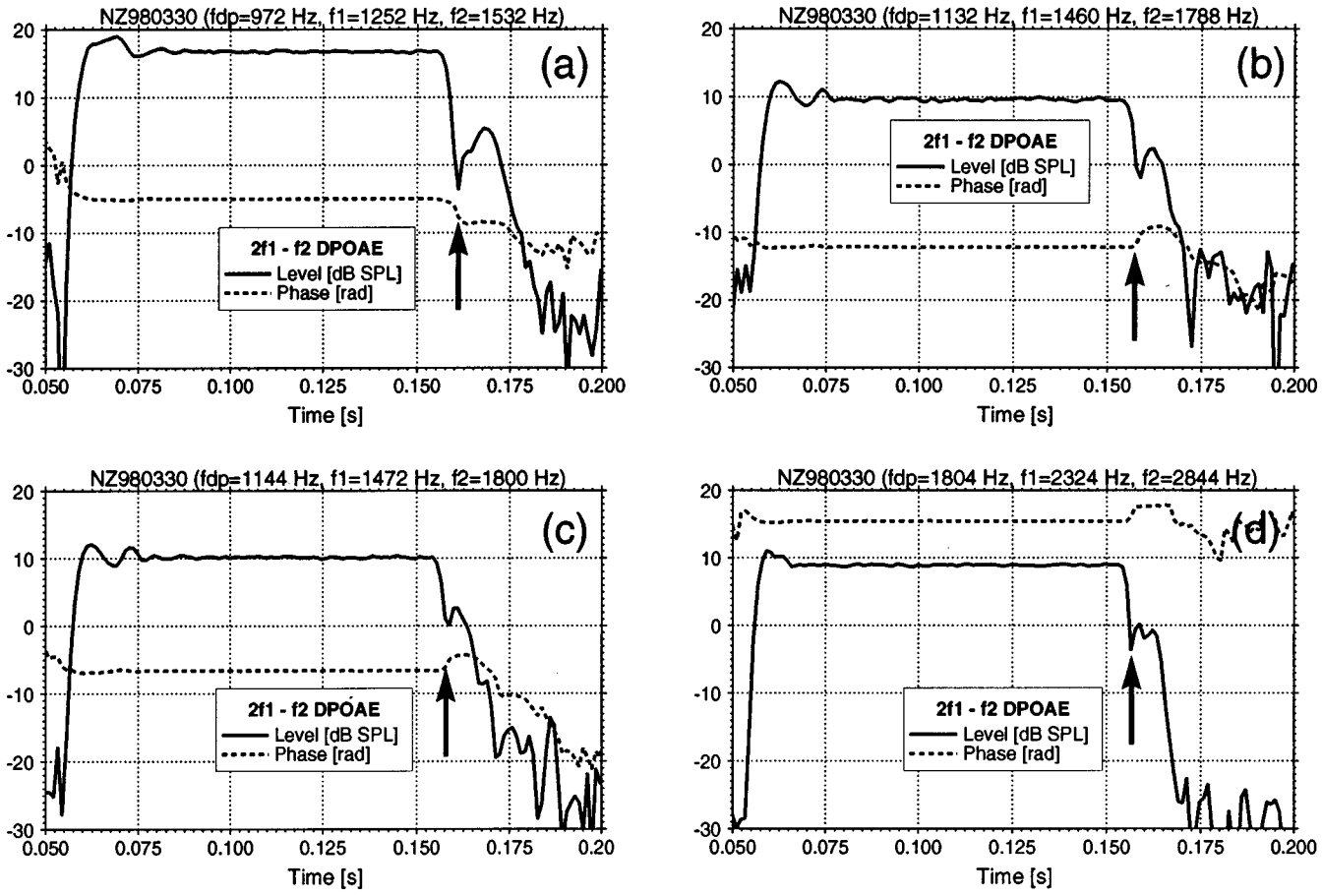

FIG. 9. 2 f_1-f_2 DPOAE level and phase as a function of time for subject NZ for various choices of f_{dp}. The frequency ratio and levels of the primaries are the same as in Fig. 6. The arrows point to the interference notch discussed in Sec. IV C.

during the first 15 min after the subject was placed in the booth in order to reduce this variability.) The variability of the DPOAE amplitude fine structure observed in these experiments (e.g., compare Figs. 6 and 9, and Figs. 7 and 10) is exaggerated by the fact that many of the measurements were obtained near deep DPOAE amplitude fine-structure minima. Because the levels of the two DPOAE components are nearly equal for deep minima, any small variation in either component will cause a small frequency shift in the location of the minimum in these cases. This small shift in the minimum location results in large DPOAE amplitude changes when the frequencies used in the measurements are held fixed.

In addition to providing evidence for the two-source model, the pulsed DPOAE paradigm provides a basis for evaluation of the latency, phase, and amplitude of each of the components. There is a frequency-specific shift in the onset of the response (the onset latencies increase with decreasing f_2). Rough estimates of latency can be obtained by observing the time-to-peak amplitude for the initial and final bursts. Accurate estimates of the latencies of the two components depend on fitting the pulsed DPOAE data to a model of the components from the two sources and their reflections [e.g., Eq. (27)]. A similar model can be applied to the continuous-tone data to extract the levels and phases of the two components. The results of these analyses will be presented in a later paper.

Group delay has been used to estimate travel times for DPOAEs (cf. Bowman *et al.*, 1997). The frequency of one of the primaries is swept over a narrow range and the group delay extracted from the slope of the phase is taken as an estimate of the travel time to and from the place of DPOAE generation. The estimate of latencies obtained in this manner is used as the basis for speculations concerning the mechanisms underlying DPOAEs. This procedure may be very misleading. The steady-state DPOAE phase may be dominated by the component from the reflection site and, in general, the interpretation of the group delay is complicated by the presence of two cochlear sources of DPOAEs, which results in the group-delay fine structure reported upon in this study.

V. STUDY 3: THE USE OF SUPPRESSION TO MANIPULATE THE RELATIVE LEVELS OF THE TWO SOURCES

A suppressor tone with a frequency close to that of the DPOAE should have a larger effect on the amplitude of the reflection-site DPOAE component than on that of the nonlinear-overlap-region component (Kummer *et al.*, 1995; Gaskill and Brown, 1996; Heitmann *et al.*, 1998). It should thus be possible to manipulate the relative levels of the two components by the addition of such a suppressor tone. As the

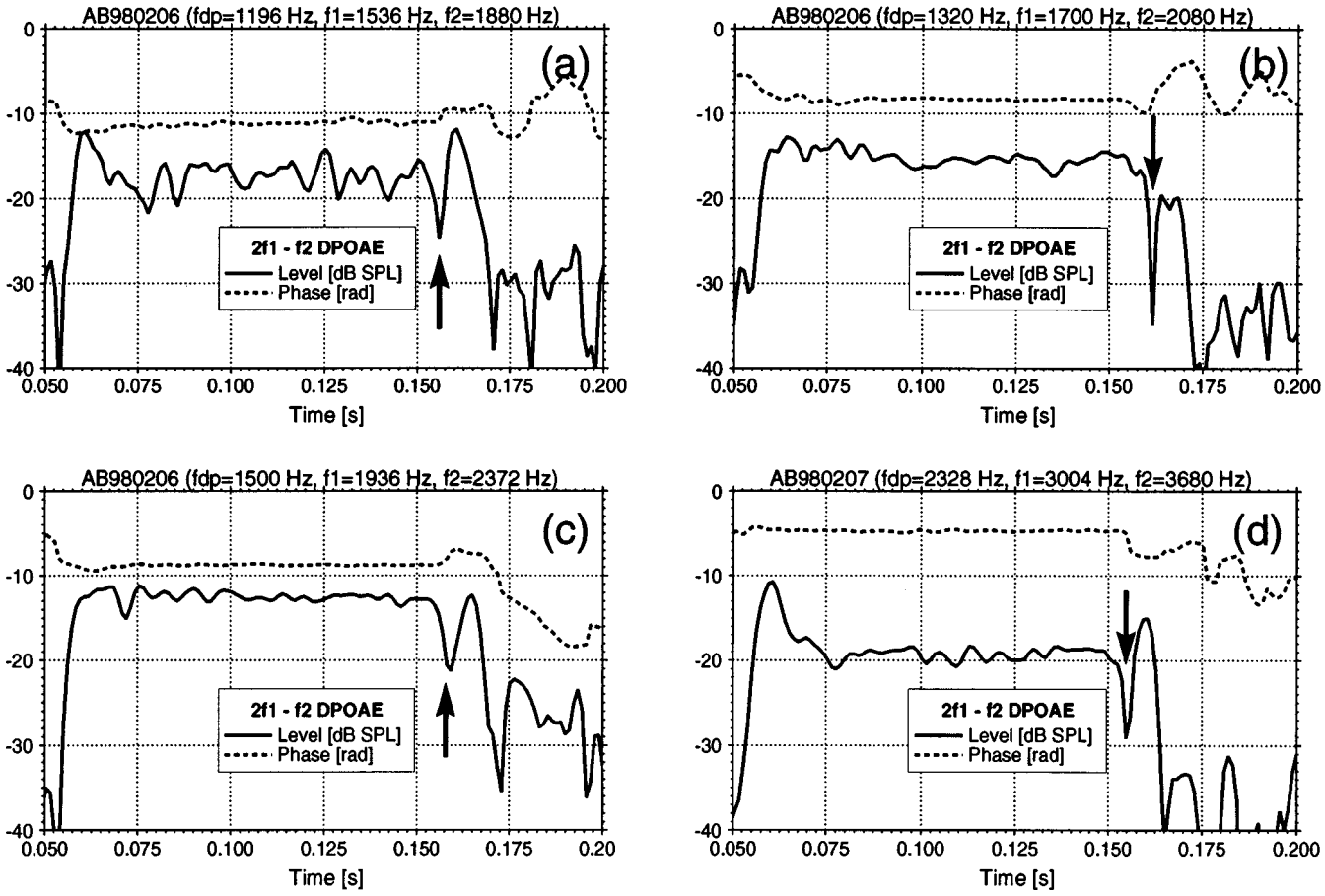

FIG. 10. 2 f_1-f_2 DPOAE level and phase as a function of time for subject AB for various choices of f_{dp}. The frequency ratio and levels of the primaries are the same as in Fig. 7. The arrows point to the interference notch discussed in Sec. IV C.

suppressor tone increases in level, it will initially have no noticeable effect, but will then reduce a_{refl} without significantly changing a_{nl}. Further increases in the level of the third tone will eventually suppress a_{nl} and the overall level of the DPOAE. The position of the notch in the pulsed-tone paradigm should shift from the beginning to the end of the pulsed response (e.g., Fig. 3) when there is a transition from a ramp-like to a rounded saw-tooth phase function (e.g., Fig. 2) in the fixed-ratio sweeps with increasing suppressor level.

The model predicts that multiple interference notches will occur after f_2 signal turn-off if the internal reflection is large enough for the observation of multiple internally reflected components, and if each successive component arrives at the stapes out of phase with the previous component. If the model prediction is correct, then complete suppression of the reflection-site DPOAE component will not only remove the DPOAE fine structure, but will obliterate the trailing interference notches associated with multiple internal reflection.

A. Methods

1. Continuous primaries

Detailed fixed-ratio measurements were made in some of the fine-structure regions with the inclusion of a suppressor tone. For most of the measurements, the frequency of the suppressor tone was located 24 Hz above that of the 2 f_1-f_2 DPOAE, and measurements over the entire frequency range were made for suppressor levels typically ranging from 10 to 80 dB SPL (see Heitmann *et al.*, 1998). The range in levels of the suppressor tone was chosen so that the effect on fine structure ranged from no significant effect (lowest levels) to obliteration of the fine structure (highest levels).

2. Pulsed primary

In order to use the pulsed-tone paradigm with suppression and still permit the clear resolution of the pulsed DPOAE and the suppressor tone, the suppressor tone was shifted to approximately 300 Hz below that of the DPOAE. The primary frequencies were once again chosen to cover a range of DPOAE levels which include two maxima and a single minimum. After the continuous-tone data had been obtained, a DPOAE frequency which corresponds to a DPOAE level greater than 10 dB above the amplitude minimum was chosen for the pulsed primary paradigm to produce the clearest representations of the (destructive) interference of the two DPOAE components. Two suppressor levels were used for the pulsed-tone paradigm: One was 10 dB lower in level and one was 10 dB higher in level than that needed to produce the transition. A smaller number of replications of the pulsed tone paradigm was obtained in order to allow all of the data from the various paradigms to be collected over a period of 1 1/2 h.

A specific test of the hypothesis that the trailing pulses expected from the model (e.g., Fig. 4), observed in some of

the experimental measurements originated from multiple internal reflection of the DP wave, was performed for subject ER for $2f_1-f_2=1908$ Hz, $f_2/f_1=1.225$, $L_1=65$ dB SPL, $L_2=55$ dB SPL for a suppressor 318 Hz below the frequency of the DPOAE with suppressor levels ranging from 10 to 75 dB SPL. This frequency region was selected because large DPOAE pulses were observed in the pulsed-primary-tone measurements.

B. Results

1. Continuous primaries

Two effects of the third tone on the level and phase of the fine structure were seen. If the phase behavior was a rounded saw-tooth in the absence of suppression (Fig. 11), then increasing the level of the suppressor tone reduced the phase and amplitude fine structure. At the highest suppression levels, the level and phase of the DPOAE both changed slowly with frequency. On the other hand, when the phase had a localized steep slope (ramp-like) around the amplitude minimum (Figs. 12 and 13) the initial effect of increasing suppressor-tone level was to deepen the amplitude fine structure and increase the phase slope at the amplitude minimum. Further increases of the suppressor tone reduced the amplitude fine structure and changed the phase behavior to a rounded sawtooth fluctuation.

2. Pulsed primary

The effects of increasing the level of a suppressor tone 316 Hz below the DP frequency are shown in Fig. 14. The DPOAE frequency was swept from 1760–1850 Hz for suppressor levels from 20 to 60 dB SPL in 10-dB steps. A more intense suppressor level (60 dB SPL) was needed to produce a transition in the phase behavior than was needed when the suppressor-tone frequency was only 24 Hz above that of the DPOAE (40 dB SPL). The change in phase behavior was associated with the deepest amplitude minimum. Once the suppressor levels necessary to produce this change in phase behavior were established, two primary frequencies were chosen so as to produce a DPOAE near the fine-structure minimum ($f_1=2323$ Hz, $f_2=2846$ Hz, $2f_1-f_2=1800$ Hz), and the pulsed f_2 paradigm was conducted with suppressor tones (1482 Hz) of 40 and 60 dB SPL.

When the 40-dB SPL suppressor was used, the notch in the pulsed DPOAE amplitude occurred near the turn-on of the pulsed f_2 tone [Fig. 15(a)], and the phase behavior was ramp-like [Fig. 14(b)]. On the other hand, when the 60-dB SPL suppressor was used, the notch in the pulsed DPOAE amplitude was shifted to shortly after the turn-off of the pulsed f_2 tone [Fig. 15(b)] and the phase behavior was rounded saw-toothed [Fig. 14(b)]. The 60-dB suppressor tone also eliminated the three additional secondary pulses after f_2 turn-off which were present in the case of the 40-dB SPL suppressor.

Suppression of the secondary pulses was also noted in other pulsed-tone suppression experiments. Representative data from these measurements are shown in Fig. 16 for $L_s=20$ dB SPL and $L_s=70$ dB SPL. These data are much noisier than most of the earlier data because they were obtained with just 32 s of data per presentation conditions. However, two secondary pulses are readily observable in Fig. 16(a), but are suppressed below the noise floor in Fig. 16(b).

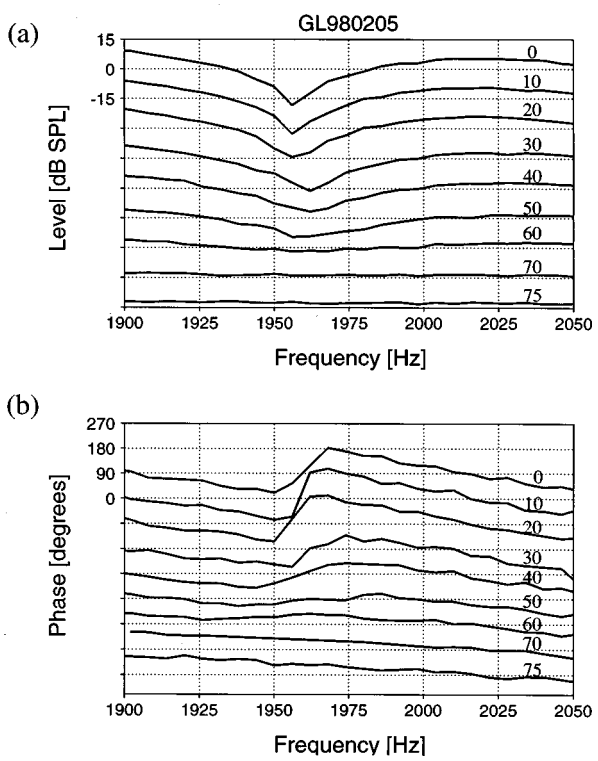

FIG. 11. Amplitude (a) and phase (b) of the $f_{dp}=2f_1-f_2$ DPOAE for $f_2/f_1=1.225$, and suppressor frequency $f_s=f_{dp}=24$ Hz for subject GL. The curves for successive levels of suppression (indicated on the right-hand end of each curve) are shifted downwards by 15 dB for (a) and by 90 deg for (b). Note that both the level minimum and the ''step'' in phase are eliminated for high suppressor levels.

C. Discussion

1. Continuous primaries

Figure 11 shows an example of the suppression of the DPOAE fine structure of a subject for which $a_{\text{refl}}<a_{\text{nl}}$ for the unsuppressed case [compare with Fig. 2(b)]. For this case, increasing the suppressor level removes the amplitude fine structure, and flattens the phase function (which in all cases would exhibit a rounded saw-tooth behavior).

Figures 12 and 13 provide examples where $a_{\text{refl}}>a_{\text{nl}}$ for the unsuppressed case [compare with Fig. 2(d)]. Here, increasing the suppressor level (10–30 dB SPL for Figs. 12 and 10, 20 dB SPL for Fig. 13) initially makes a_{refl} become approximately equal to a_{nl} and consequently deepens the amplitude fine structure. The phase behavior remains ramp-like, with an increasing slope with increasing suppressor level. Once the suppressor is high enough in level (40–70 dB SPL for Fig. 12 and 30–60 dB SPL for Fig. 13), a_{refl} becomes less than a_{nl}, the amplitude fine structure begins to decrease, and eventually disappears. A categorical shift in phase behavior from ramp-like to rounded saw-tooth-like behavior is also seen. Further increases in the suppressor level causes the phase function to flatten as in the first case described above. For high-enough suppressor levels (>70 dB SPL in Fig. 12),

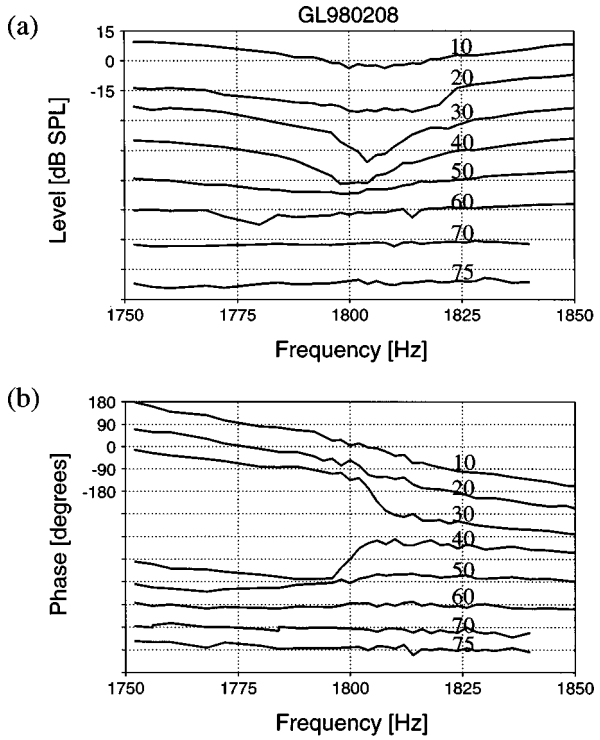

FIG. 12. Amplitude (a) and phase (b) of the $f_{dp}=2f_1-f_2$ DPOAE for $f_2/f_1=1.225$, and suppressor frequency $f_s=f_{dp}+24$ Hz for subject GL. The curves for successive levels of suppression (indicated on the right-hand end of each curve) are shifted downwards by 15 dB for (a) and by 90 deg for (b). Note that the level minimum initially deepens before becoming more shallow as the suppressor level is increased. Additionally, the phase behavior transitions from a ramp-like function to a step-like function as the suppressor level is increased.

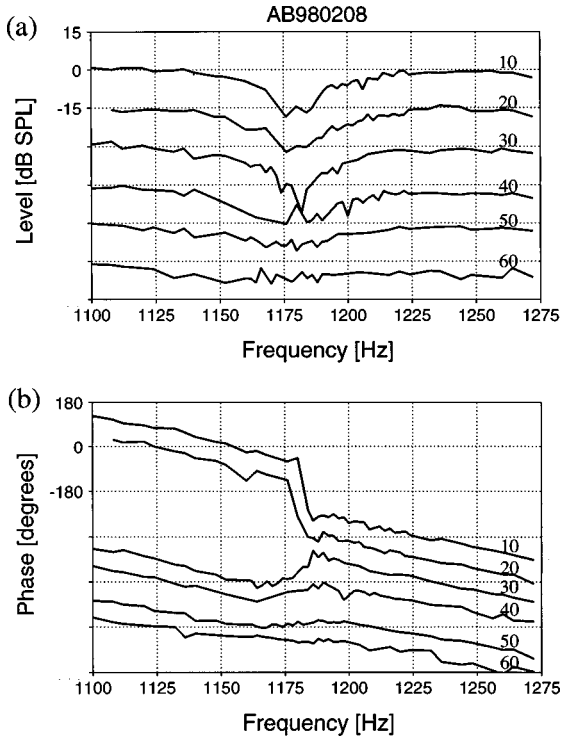

FIG. 13. Amplitude (a) and phase (b) of the $f_{dp}=2f_1-f_2$ DPOAE for $f_2/f_1=1.225$, and suppressor frequency $f_s=f_{dp}+24$ Hz for subject AB. The curves for successive levels of suppression (indicated on the right-hand end of each curve) are shifted downwards by 15 dB for (a) and by 90 deg for (b).

both the reflection-site and the overlap-region components are suppressed, and the overall level of the DPOAE decreases. The ability to predictably change the correlation between group delay and amplitude fine structure by suppressing the component from the DP site provides additional evidence for our two-source theory.

2. Pulsed primary

Figure 15 provides an example in which a direct manipulation (the inclusion of a suppressor tone) is able to shift the behavior of the phase from ramp-like (associated with $a_{refl}>a_{nl}$) to rounded saw-tooth-like, and is able to shift (in a predictable fashion) the location of the interference notch between the two source components from shortly after the f_2 signal turn-on until shortly after f_2 turn-off. The ability to predict the position of the notch in the pulsed DPOAE data from the phase characteristics of the continuous data (with and without suppression) provides a rigorous test of the two-source model.

As predicted, the suppressor tone not only changed the position of the notch for subject GL, but also eliminated the sequences of bursts after stimulus turn-off [see Fig. 15(b)]. There can be reflections even if $a_{nl}>a_{refl}$ and the notch is at the end of a pulse [see Fig. 16(a)]. The addition of a suppressor tone reduces a_{refl} to the noise floor and removes the bursts of predictable amplitude and phase following stimulus turn-off [see Fig. 16(a)].

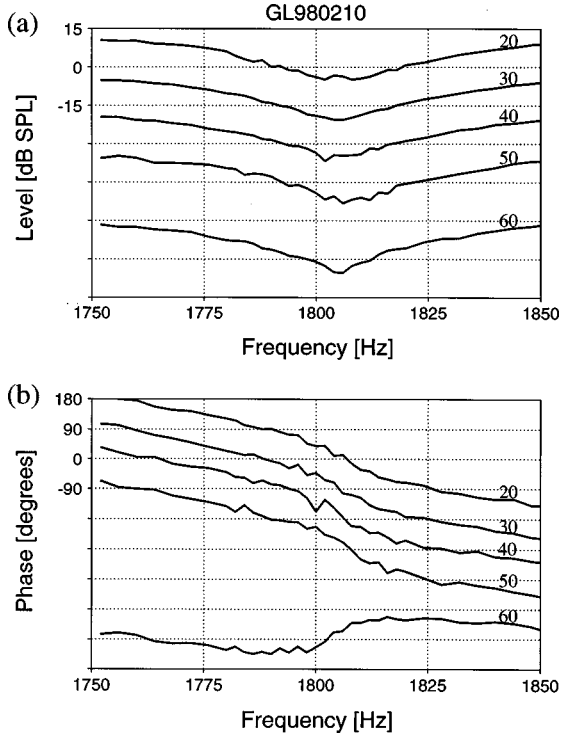

FIG. 14. Amplitude (a) and phase (b) of the $f_{dp}=2f_1-f_2$ DPOAE for $f_2/f_1=1.225$, and suppressor frequency $f_s=f_{dp}-300$ Hz for subject GL. The curves for successive levels of suppression (indicated on the right-hand end of each curve) are shifted downwards by 15 dB for (a) and by 90 deg for (b).

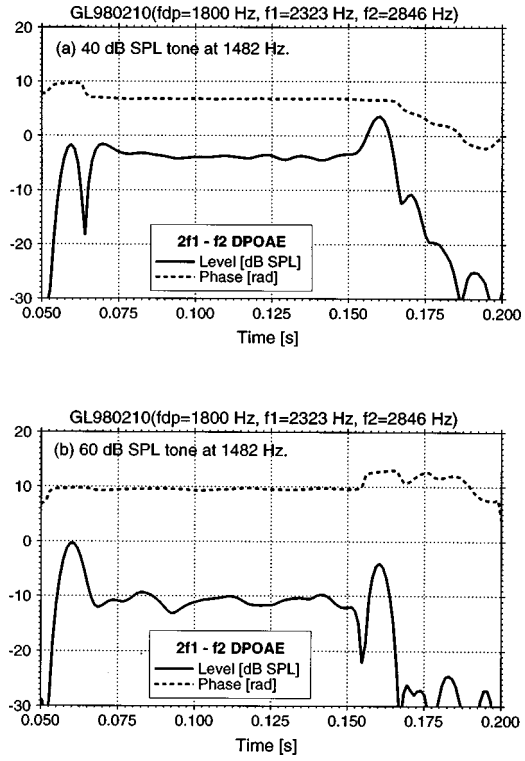

FIG. 15. $2f_1-f_2$ DPOAE level and phase as a function of time for $f_{dp}=1800$ Hz, $f_2/f_1=1.225$, $L_1=65$ dB SPL, and $L_2=55$ dB SPL for subject GL on the same day and conditions as Fig. 14. A suppressor tone at 1482 Hz was 40 dB SPL in (a) and 60 dB SPL in (b). Note the movement of the notch from the onset (a) to the offset (b) of the DPOAE at levels of the suppressor which produce a change in the phase behavior at the amplitude minimum in Fig. 14.

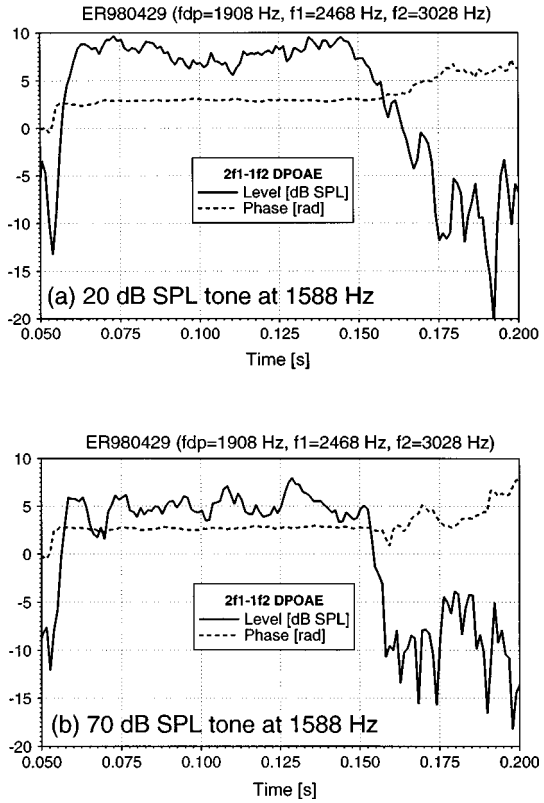

FIG. 16. $2f_1-f_2$ DPOAE level and phase as a function of time for $f_{dp}=1908$ Hz, $f_2/f_1=1.225$, $L_1=65$ dB SPL, and $L_2=55$ dB SPL for subject ER. A suppressor tone at 1588 Hz was 20 dB SPL in (a) and 70 dB SPL in (b). Note the disappearance of the train of secondary pulses in (b).

VI. CONCLUSIONS

A model of DPOAEs as the sum of two sources permits the prediction of the outcome of three different experimental paradigms and the evaluation of the relative amplitudes and latencies of the two source components. The pattern of the fixed-ratio sweeps (within each experimental session) permitted the prediction of the pattern of results for the other two experimental paradigms.

When the spacing between adjacent DPOAE frequencies with a fixed frequency-ratio paradigm was made fine enough to unambiguously determine the total phase of the DPOAE, the patterns of DPOAE amplitude fine structure, phase variation, and group-delay fine structure agreed with those expected from the model of Talmadge *et al.* (1998). In some cases, the patterns of amplitude fine structure, phase variation, and group-delay fine structure are consistent with amplitude dominance of the overlap-region component, and in other cases, with the dominance of the component from the DP tonotopic place.

Measurements of the time courses of the amplitude and phase of DPOAEs were extracted from a paradigm in which the DPOAE is pulsed by pulsing the f_2 primary tone on and off, while keeping the f_1 primary tone continuous in level. Under circumstances in which the overlap-region component is expected to be dominant from fixed-ratio measurements, an interference notch is observed in the DPOAE amplitude shortly after turn-off of the f_2 primary, as expected from the theory. Similarly, when the DP tonotopic-place component is expected to be dominant from fixed-ratio measurements, an interference notch is observed in the DPOAE amplitude shortly after turn-on of the f_2 primary.

By introducing a suppressor tone near in frequency to the DPOAE, a transition was brought about in the patterns of amplitude, phase, and group delay from those in which the reflection-site component is dominant to patterns in which the overlap-region component is dominant. Furthermore, it was possible to shift the location of the interference null until after turn-off of the f_2 primary, consistent with the theory.

It is important to note that the degree of specificity of predictions given in this paper can only be given by a *detailed* two-source model. Simply positing that two sources exist, without a detailed mathematical description of their origins and amplitude and phase behavior with ω_1, ω_2, and ω_{dp}, is not sufficient to give rise to unique predictions for either continuous-tone or pulse-tone DPOAE measurements. For example, papers such as Kemp and Brown (1983), Gaskill and Brown (1996), and Heitmann *et al.* (1998), which suggested the possibility of a two-source origin for DPOAEs, did not give rise to well-defined predictions for the fixed frequency-ratio experiments, the pulsed-DP experiments, and especially did not predict the relationship between the two experimental paradigms reported in this study. In order for a two-source model to reproduce the phenomenology reported in this study, it is necessary that the model give a complete description of how the second (reflection-

site) source varies in phase with the DPOAE frequency, and this was not done in these earlier studies.

ACKNOWLEDGMENTS

We would like to thank Christopher Tong for reading this manuscript. This research was supported in part by the NIH/NIDCD grant No. R29 DC03094.

Bowman, D. M., Brown, D. K., Eggermont, J. J., and Kimberley, B. P. (**1997**). ''The effect of sound intensity on $f1$-sweep and $f2$-sweep distortion product otoacoustic emissions phase delay estimates in human adults,'' J. Acoust. Soc. Am. **101**, 1550–1559.

Brown, A. M., Harris, F. P., and Beveridge, H. A. (**1996**). ''Two sources of acoustic distortion products from the human cochlea,'' J. Acoust. Soc. Am. **100**, 3260–3267.

Gaskill, S. A., and Brown, A. M. (**1996**). ''Suppression of human acoustic distortion product: dual origin of $2f_1-f_2$,'' J. Acoust. Soc. Am. **100**, 3268–3274.

Gorga, M. P., Neely, S. T., BM, B. M. B., Beauchaine, K. L., Kaminski, J. R., and Liu, Z. (**1994**). ''Towards understanding the limits of distortion product otoacoustic emission measurements,'' J. Acoust. Soc. Am. **96**, 1494–1500.

Greenwood, D. D. (**1990**). ''A cochlear frequency position function for several species—29 years later,'' J. Acoust. Soc. Am. **87**, 2592–2605.

Heitmann, H. J., Waldmann, B., Schnitzler, H. U., Plinkert, P. K., and Zenner, H.-P. (**1997**). ''Suppression growth functions of DPOAE with a suppressor near $2f1-f2$ depends on DP fine structure: Evidence for two generation sites for DPOAE,'' in *Abstracts of the Twentieth Midwinter Research Meeting of the Association for Research in Otolaryngology*, edited by G. R. Popelka (Association for Research in Otolaryngology, Des Moines, IA), p. 190.

Heitmann, J., Waldmann, B., and Plinkert, P. K. (**1996**). ''Limitations in the use of distortion product otoacoustic emissions in objective audiometry as the result of fine structure,'' European Archives of Otolaryngology **253**, 167–171.

Heitmann, J., Waldmann, B., Schnitzler, H. U., Plinkert, P. K., and Zenner, H. P. (**1998**). ''Suppression of distortion product otoacoustic emissions (dpoae) near $2f(1)=f(2)$ removes *dp*-gram fine structure—evidence for a secondary generator,'' J. Acoust. Soc. Am. **103**, 1527–1531.

Kemp, D. T. (**1979**). ''The evoked cochlear mechanical response and auditory microstructure—evidence for a new element in cochlear mechanics,'' Scand. Audiol. Suppl. **9**, 35–47.

Kemp, D. T., and Brown, A. M. (**1983**). ''An integrated view of the cochlear mechanical nonlinearities observable in the ear canal,'' in *Mechanics of Hearing*, edited by E. de Boer and M. A. Viergever (Martinus Nijhoff, The Hague, The Netherlands), pp. 75–82.

Kummer, P., Janssen, T., and Arnold, W. (**1995**). ''Suppression tuning characteristics of the $2f_1-f_2$ distortion product otoacoustic emission in humans,'' J. Acoust. Soc. Am. **98**, 197–210.

Liberman, M., Puria, S., and Guinan, J. J. (**1996**). ''The ipsilaterally evoked olivocochlear reflex causes rapid adaptation of the $2f1-f2$ distortion product otoacoustic emission,'' J. Acoust. Soc. Am. **949**, 3572–3584.

Long, G. R., and Talmadge, C. L. (**1997**). ''The frequency of spontaneous otoacoustic emissions is modulated by heartbeat,'' J. Acoust. Soc. Am. **102**, 2831–2848.

Martin, G. K., Jassir, D., Stagner, B. B., Whitehead, M. L., and Lonsbury-Martin, B. (**1998**). ''Locus of generation for the $2f12\,f2$ vs $2f22\,f1$ distortion-product otoacoustic emissions in normal-hearing humans revealed by suppression tuning, onset latencies, and amplitude correlations,'' J. Acoust. Soc. Am. **103**, 1957–1971.

Mathews, J., and Walker, R. (**1964**). *Mathematical Methods of Physics* (Benjamin, New York).

Mills, D. M. (**1997**). ''Interpretation of distortion product otoacoustic emission measurements: I. Two stimulus tones,'' J. Acoust. Soc. Am. **102**, 413–429.

Piskorski, P. (**1997**). ''The origin of the distortion product otoacoustic emission fine structure,'' Ph.D. thesis, Purdue University, West Lafayette, IN.

Robinette, M. S. and Glattke, T. J., editors (**1997**). *Otoacoustic Emissions: Clinical Applications* (Thieme, New York).

Shera, C. A., and Zweig, G. (**1993**). ''Order from chaos: Resolving the paradox of periodicity in evoked otoacoustic emission,'' in *Biophysics of Hair Cell Sensory Systems*, edited by H. Duifhuis, J. W. Horst, P. van Dijk, and S. M. van Netten (World Scientific, Singapore), pp. 54–63.

Siegel, J., and Hirohata, E. (**1994**). ''Sound calibration and distortion product otoacoustic emissions at high frequencies,'' Hearing Res. **80**, 146–152.

Stover, L. J., Neely, S. T., and Gorga, M. P. (**1996**). ''Latency and multiple sources of distortion product emissions,'' J. Acoust. Soc. Am. **99**, 1016–1024.

Sun, X. M., Schmiedt, R. A., He, N.-J., and Lam, C. F. (**1994a**). ''Modeling the fine structure of the $2f(1)-f(2)$ acoustic distortion product. I. Model development,'' J. Acoust. Soc. Am. **96**, 2166–2174.

Sun, X. M., Schmiedt, R. A., He, N.-J., and Lam, C. F. (**1994b**). ''Modeling of the fine structure of the $2f(1)-f(2)$ acoustic distortion product. II. Model evaluation,'' J. Acoust. Soc. Am. **96**, 2175–2183.

Talmadge, C., Long, G. R., and Tubis, A. (**1993**). ''New off-line method for detecting spontaneous otoacoustic emissions in human subjects,'' Hearing Res. **71**, 170–182.

Talmadge, C., Tubis, A., Long, G. R., and Piskorski, P. (**1998**). ''Modeling otoacoustic emission and hearing threshold fine structures in humans,'' J. Acoust. Soc. Am. **104**, 1517–1543.

Talmadge, C., Tubis, A., Piskorski, P., and Long, G. R. (**1997**). ''Modeling otoacoustic emission fine structure,'' in *Diversity in Auditory Mechanics*, edited by E. Lewis, G. Long, R. Lyon, P. Narins, and C. Steele (World Scientific, Singapore), pp. 462–471.

Talmadge, C. L., Tubis, A., Long G. R., and Piskorski, P. (**1996**). ''Evidence for multiple spatial origins of the fine structure of distortion product otoacoustic emissions in humans, and its implications: Experimental and modeling results,'' in Abstracts of the Nineteenth Midwinter Research Meeting of the Association for Research in Otolaryngology, edited by D. J. Lim (unpublished), p. 94. Abstract.

Whitehead, M. L. (**1991**). ''Slow variations of the amplitude and frequency of spontaneous otoacoustic emissions,'' Hearing Res. **53**, 269–280.

Whitehead, M., Stagner, B., Martin, G., and Lonsbury-Martin, B. (**1995**). ''Effects of ear-canal standing waves on measurements of distortion-product otoacoustic emissions,'' J. Acoust. Soc. Am. **98**, 3200–3214.

Whitehead, M., Stagner, B., Martin, G., and Lonsbury-Martin, B. (**1996**). ''Visualization of the onset of distortion-product otoacoustic emissions, and measurement of their latency,'' J. Acoust. Soc. Am. **100**, 1663–1679.

Zweig, G. (**1991**). ''Finding the impedance of the organ of Corti,'' J. Acoust. Soc. Am. **89**, 1229–1254.

Zweig, G., Lipes, R., and Pierce, J. R. (**1976**). ''The cochlear compromise,'' J. Acoust. Soc. Am. **59**, 975–982.

Zweig, G., and Shera, C. A. (**1995**). ''The origins of periodicity in the spectrum of evoked otoacoustic emissions,'' J. Acoust. Soc. Am. **98**, 2018–2047.